ACSNANO

Nanocrystal Quantum Dots: From Discovery to Modern Development

Alexander L. Efros* and Louis E. Brus*

Cite This: *ACS Nano* 2021, 15, 6192−6210

Read Online

ACCESS | Metrics & More | Article Recommendations

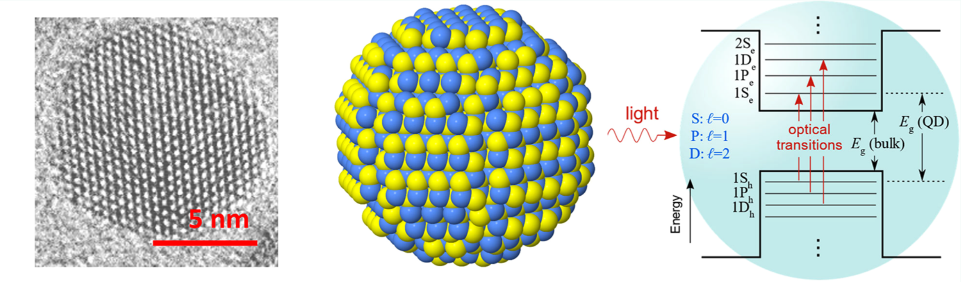

TEM image of CdSe nanocrystal   Nanocrystal atomic structure

ABSTRACT: **This review traces nanocrystal quantum dot (QD) research from the early discoveries to the present day and into the future. We describe the extensive body of theoretical and experimental knowledge that comprises the modern science of QDs. Indeed, the spatial confinement of electrons, holes, and excitons in nanocrystals, coupled with the ability of modern chemical synthesis to make complex designed structures, is today enabling multiple applications of QD size-tunable electronic and optical properties.**

KEYWORDS: *nanocrystals, quantum dots, quantum dot synthesis, colloid, exciton, quantum size effect, core−shell structures, liquid crystal display, light-emitting diodes, solar cells*

Semiconductor nanocrystals (NCs) are the most heavily studied of the nanoscale semiconductors, and now we have a solid, theoretical basis that allows us to understand most of their electronic, optical, and transport properties. It was nearly 4 decades ago when Alexei Ekimov and Alexander Efros, working at the S. I. Vavilov State Optical Institute and A. F. Ioffe Institute, Russia, began studying semiconductor-doped glasses and developing theories to explain their observed properties. Simultaneously, but half a world away, Louis Brus at Bell Laboratories in Murray Hill, NJ, was investigating semiconductor particles in liquid colloids. These two lines of research, separated both geographically and by the Iron Curtain, eventually led to the two groups' independent development of NCs and theoretical explanation of their size-dependent optical properties.[1−15] It was not until 1984, however, that the Americans learned of the Russians' efforts, when Brus read translations of the Ekimov papers and wrote to the author. An additional 5 years had to pass before the researchers could begin their intensive information exchange after the fall of the Iron Curtain and the introduction of *Glasnost and Perestroika* in Russia.

Despite obvious differences between semiconductor-doped glasses and semiconductor colloidal dispersions, it was shown that in both cases, NC growth resulted from a diffusion-controlled microscopic precipitation process. Control over this process allowed NC size to be varied over a wide range, the smallest of which were only a few nanometers. Since that time, NCs of almost all semiconductor materials have been successfully grown, and many interesting physical phenomena have been reported. In liquid colloids, a vast improvement in NC quality and structure has been achieved since then using the synthetic methods and ideas of modern chemistry.

Over the years it has been established that the size dependence of NC absorption and luminescence spectra is determined by carrier spatial confinement, which drastically modifies the energy spectra of three-dimensionally confined electrons, holes, and excitons. The energy of the lowest quantum confinement levels of electrons and holes increases with

Received: February 15, 2021
Accepted: April 1, 2021
Published: April 8, 2021

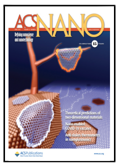

ACS Publications

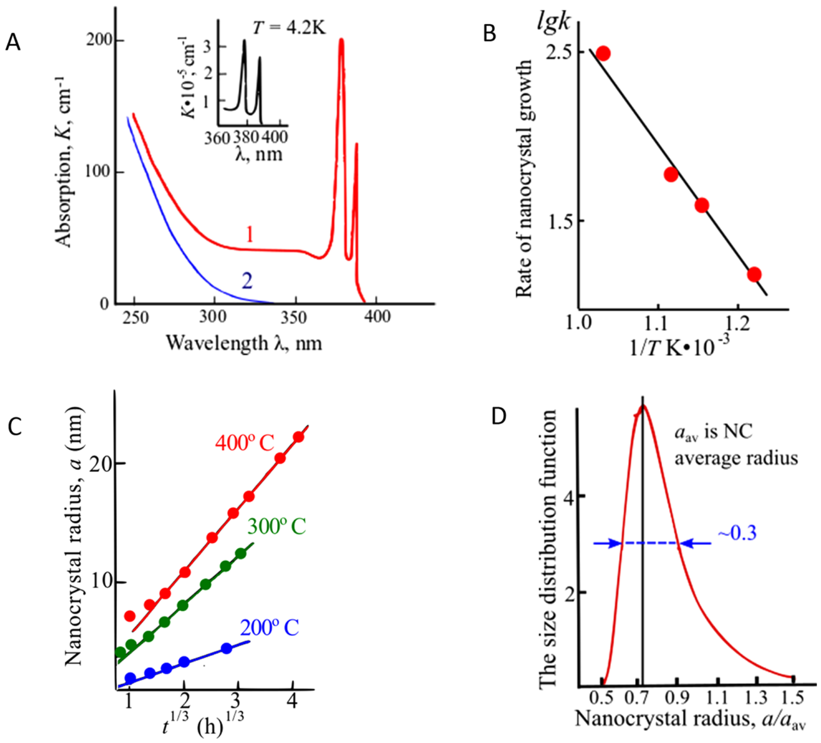

Figure 1. Nucleation and growth of CuCl NCs in a glass. (A) Low-temperature absorption spectra of CuCl activated glass (1) and of pure glass (2) both annealed at 700 °C for 1 h. Inset shows the absorption spectra of bulk CuCl. Adapted with permission from ref [1]. Copyright 1980 Nauka. (B) Rate of NC growth as a function of inverse temperature. (C) Dependence of NC radius on the duration of annealing conducted at three temperatures $T = 200$, 300, and 400 °C. (B and C) Adapted with permission from ref [2]. Copyright 1981 Nauka. (D) Universal distribution of NC sizes creating during Ostwald ripening stage of NC growth described by Lifshitz and Slyosov.[25]

decreasing NC size and increases the energy of the band edge optical transitions.[3−9] For example, in CdSe NCs, this shift of the energy gap can be as large as 1.2 eV.[16,17] By changing size, it is possible to vary the energy gap of this material from 1.8 eV (its bulk value) to 3 eV, encompassing nearly the entire visual range of the optical spectrum. This size tunability of electronic and optical properties leads to diverse applications.

Modern NC research generates knowledge and materials that are important to the massive worldwide computer/communications electronics industry. There have been demonstrations of tunable, room-temperature lasing using NC solids and of prototype NC-based light-emitting diodes (LEDs) and photovoltaic cells as well as commercial products in NC quantum dot (QD) biolabeling. Periodic arrays of semiconductor NCs are solution-processable materials for low-cost, flexible, thin-film electronics, with reports that these structures can achieve a mobility of 25 cm^{2}V^{-1}s^{-1}. In 2012, researchers from Samsung Electronics demonstrated a 4 in. full-color QD display, which was brighter than previous liquid-crystal displays and consumed less than one-fifth of the power. Today Samsung and other companies sell inexpensive "QLED" liquid crystal display televisions with vivid colors, in which the green and red pixels are composed of optically excited luminescing QDs. This has become a multibillion dollar business worldwide.

NCs today are typically complex core−multishell heterostructures, often with chemically functionalized surfaces. Engineered properties can include the frequency of light emission, ability to transfer photoexcited electrons, suppression of the nonradiative recombination, shortening of the radiative decay time, doping, and/or specific solubility in various environments. We discuss some aspects of how these properties are controlled and list several important developments and insights. Other reviews go into greater depth in specific aspects.[18] There are also a number of monographs and journal special editions.[19−24]

We try to present our original motivation and reasoning, as best they can be remembered. As often is the case in research, we describe the roles played by curiosity, observation, theoretical modeling, persistence in the face of skepticism, and an enthusiastic readiness to engage in thoughtful contemplation of unexpected results.

SEMICONDUCTOR NCs IN GLASSES

The technology of colloidal particle growth in glass is a thousand years old. It was developed during the Middle Ages to provide the stained glasses that were used in the windows of medieval churches. The various colors of stained glass result from the homogeneously distributed inclusion of small particles of some metals, metal oxides, and even semiconductors.

In modern times, physicists use such colored glasses as optical filters (so-called Schott glasses), and it was well understood that the optical properties of these glasses activated by the halogens are determined by "colloidal particles" dispersed in a glass matrix. Interestingly, the preparation protocols for these glasses partially originate from ancient alchemy books: put such and such compounds in the glass melt, cool the melt down to such and such a temperature, then heat it up and keep it at such and such a temperature for a particular period of time. These procedures were completely empirical.

In 1979, Ekimov began working at the S. I. Vavilov State Optical Institute, which was equipped with the technology necessary for Schott glass growth. Emergence of various colors

https://doi.org/10.1021/acsnano.1c01399

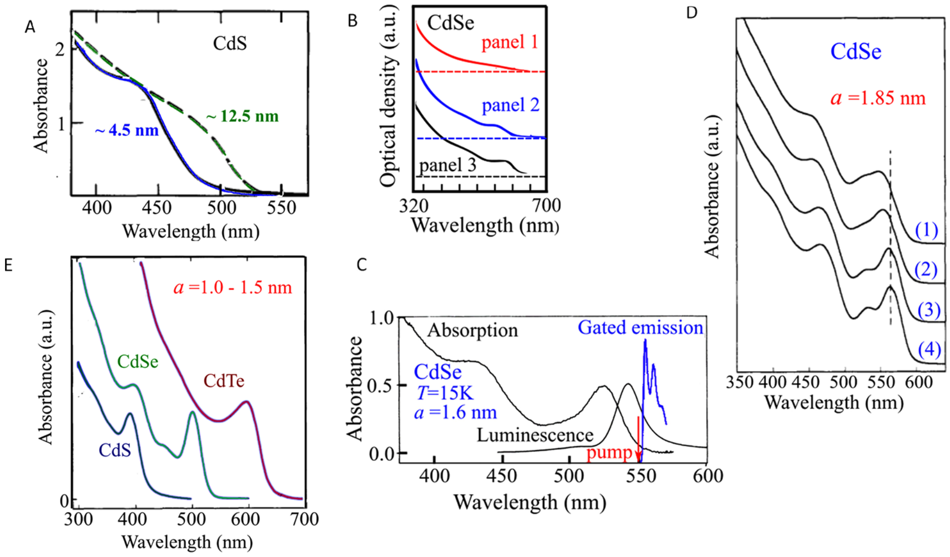

Figure 2. Nucleation and growth of NCs in an aqueous solution. (A) Room-temperature absorption spectra of "fresh" and aged for 1 day CdS NC in aqueous solution. Adapted with permission from ref 5. Copyright 1983 AIP Publishing. (B) Room-temperature absorption spectra of CdSe NC grown by inverse micelle approach, before (panel 1) and after (panel 2) postreaction annealing as well as wurtzite CdSe NCs resulting from high-temperature refluxing (panel 3). Adapted with permission from ref 39. Copyright 1989 AIP Publishing. (C) Photoluminescence from 1.6 nm radius CdSe NC and its resonance photoexcitation. Adapted with permission from ref 41. Copyright 1990 American Physical Society. (D) Absorption spectra of CdS, CdSe, and CdTe NCs. (E) Sharpening of CdSe NC absorption spectra introduced by size-selective precipitation (see modifications from (1) to (4)). (E and D) Adapted with permission from ref 17. Copyright 1993 American Chemical Society.

in semiconductor-activated glasses was a fascinating problem to look at, and Ekimov decided to investigate the underlying physicochemical mechanisms. His initial idea was to determine the structure and chemical composition of the colloidal particles and the mechanism of their growth. In contrast with the old recipes, he decided to study the effect of glass activation by a single compound. Experiments had been undertaken with glasses activated by the chloride or bromide of copper (CuCl, CuBr) as well as with glasses activated by the sulfide or selenide of cadmium (CdS, CdSe).

Ekimov's initial efforts to understand the absorption spectra of CdS and CdSe activated glasses were unsuccessful. The activation created additional broad features in the glass absorption, whose position changed significantly under various heat-treatment conditions. The first success came with the study of glasses activated by chloride of copper: CuCl. Figure 1A shows the absorption spectra of thin samples (100 μm) of glasses activated by CuCl, measured at 4.2 K. Figure 1A also shows the absorption spectra of an activated glass sample (1) and of pure glass (2), both annealed at 700C for 1 h. The spectra of the activated samples show a two-line sharp structure that is similar to the band-edge absorption of bulk CuCl crystals (see inset). In bulk CuCl, the structure was identified as two excitonic transitions connected with a spin−orbit split valence band (see inset). The similarity of both absorption spectra unambiguously showed that "colloidal" particles were simply CuCl crystalline inclusions dispersed in a glass matrix. The exciton line positions showed, however, high sensitivity to the sample-annealing temperature. A decrease of the sample-annealing temperature resulted in a larger blue shift of the excitonic structure from its bulk position.[1] This behavior suggested the existence of relationships between annealing parameters and particle size. To reveal these correlations, Ekimov and his Ph.D. mentee Alexei Onushchenko measured the mean NC radius a using small-angle X-ray scattering, for samples annealed from 500 to 700 °C, and with annealing duration varying from 1 to 96 h.[3] These measurements revealed a broad range of sizes from a = 17 Å for samples annealed at 500 °C for 4 h to a = 310 Å for samples annealed at 700 °C for 1 h. Critical assistance in understanding the various effects of annealing on NC size came from G. T. Petrovskii, Director of the Vavilov Institute. During one of his occasional visits to the laboratory, Petrovskii focused the attention of Ekimov's group on the theory of diffusion-controlled phase decomposition of oversaturated solid solutions, a theory developed by I. M. Lifshitz and V. V. Slezov.[25]

In short, their theory describes the growth of a droplet of water in air that is supersaturated by water vapors. Such a medium is unstable, and its decomposition begins with the formation of very small water droplets. As soon as these "nuclei" of the new phase are created, water begins to diffuse to the large droplets, increasing their size at the expense of the small droplets. This process, which is driven by the higher surface energy of the small droplets is known as Ostwald ripening and leads to an increase in the average droplet size over time. The same processes occur in semiconductor-activated glasses prepared by rapid cooling of the glass melt. The activated glass decomposition is controlled by the diffusion coefficient, $D = D_0 \exp(-\Delta E/kT)$, where ΔE is the activation energy of diffusion and depends exponentially on the annealing temperature, T. In such media, semiconductor NCs are the "nuclei" of a new phase. According to Lifshitz and Slyozov, the average radius of the droplet increases with annealing time, t, as $a = (4\alpha Dt/9)^{1/3}$, where α is the interfacial surface energy. This simple expression described very well the experimental dependencies of NC size on temperature (Figure 1B) and the duration (Figure 1C) of annealing. The activation energy, ΔE, was determined from the experimental results. This understanding of the thermodynamics of particle growth gave Ekimov's group a powerful tool for synthesizing NCs.

Ten years later this technique was modified to improve the dispersion of NC sizes. The steady-state dispersion of sizes created during the Ostwald ripening stage of growth is around

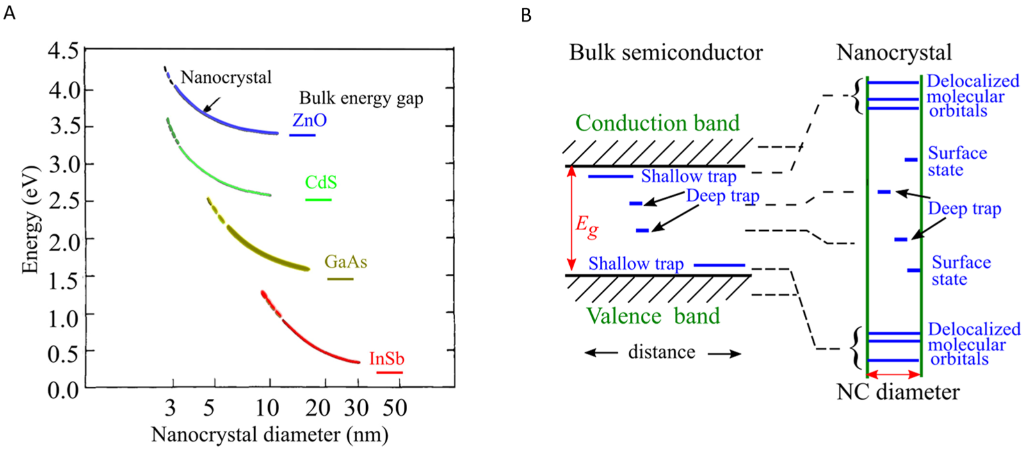

Figure 3. Theoretical ideas from the early 1980s. (A) Calculated size-dependent shift of the lowest exciton levels in strong confinement described by eq 3. Adapted with permission from ref 8. Copyright 1984 AIP Publishing. (B) Spatial electronic state correlation diagram for bulk semiconductors and NCs. Adapted with permission from ref 15. Copyright 1986 IEEE. The bulk valence and conduction bands, together with shallow trap states, evolve into the NC molecular orbitals. Deep localized defect states in the bulk have essentially the same energy in the NC. New localized surface states exist in the NC.

15% (see Figure 1D). To reduce this size dispersion, Ekimov *et al.*[16] began to use the fluctuation-mediated stage of phase decomposition for formation of QDs. Initially the glass supersaturated by the semiconductor phase was exposed to a short high-temperature treatment, during which multiple nuclei of a new phase—NCs—were created. The dispersion of NC sizes created by this means is significantly smaller than 15% because the probability of fluctuation-mediated NC formation depends exponentially on its volume. Consequent rapid cooling of the glass allows preservation of the narrow size distribution. The slow growth that follows at lower temperatures enables a change in average size, with 5% size dispersion preserved. There is a clear resemblance here to the invention of the colloidal hot-injection synthesis method more than a decade later (discussed in the following).

SEMICONDUCTOR NCs IN LIQUID COLLOIDS

The study of semiconductor particles in liquid colloids does not share the long history of stained-glass development. In the 1970s and 1980s, chemists in the United States and Europe, including Bard,[26] Fendler,[27] Gratzel,[28] and Henglein[29−31] among others, began to explore semiconductor colloids, mostly for solar energy applications. While these particles were generally too large to show confinement, Henglein did observe optical size effects and modeled them semiclassically.

Brus' initial observation of quantum size effects was accidental. In late 1982 in Murray Hill, he was studying organic photochemistry on CdS particle surfaces, using pump−probe Raman spectroscopy. He made CdS aqueous colloids by arrested precipitation following fast injection of precursor ions and observed that the CdS spectra sometimes changed with aging as Oswalt ripening occurred. He suspected that the observed change was a size effect. To confirm this idea, he slowed down the CdS NC growth by lowering precursor concentrations and decreasing the growth temperature in acetonitrile solvent, thus making smaller NCs. This allowed him to measure a blue shift and exciton peak in the absorption band edge of CdS on the freshly prepared sample (see Figure 2A). The average NC diameter was 4.5 nm, and the observed shift of absorption was consistent with an increase of the energy gap in NCs of this size due to quantum confinement of electrons and holes.[6] In aged colloids, the average NC diameter reached 12.5 nm, and the sample absorption band edge shifts back to the bulk CdS energy gap. Stimulated by these observations, Brus developed an effective mass and dielectric polarization theory that described the measured size-dependent shift.[5,8] These studies were extended to ZnS, PbS, ZnSe, CdSe, and the silver halides.[9,10,14] Two separate quantum confined excitons from a spin−orbit split valence band were observed in the spectra of ZnSe QDs precipitated at −80 °C in isopropanol. At this time, Brus inhaled a significant breath of toxic H_2Se gas when attempting to change a defective regulator on a gas tank and spent a night in the hospital.

These early synthetic approaches, and theoretical ideas outlined in Figure 3, were summarized in 1986,[15,32] just as Paul Alivisatos arrived in Murray Hill as a postdoc. It was decided to try to find better chemical methods to make and control NCs. Chemical synthesis is manpower intensive compared with spectroscopy. Thus, to initiate this program, Brus, Alivisatos, and synthetic chemist Michael Steigerwald began to work daily side-by-side, trying different synthetic ideas and adopting Schlenk vacuum line and glovebox techniques from organometallic chemistry to exclude oxygen.

Structured liquid inverse micelle solutions were explored in an attempt to control CdSe particle growth and structure. These solutions contain *ca.* 100 Å diameter water droplets with a surface surfactant layer, in bulk heptane liquid. Each droplet could be a "microreactor" containing one growing NC; NCs in different droplets are prevented from fusing with each other by the micelle structure. After initial nucleation, it was observed that if reagents for CdSe were added slowly, they would grow on existing NCs but not nucleate new NCs. This was seen in the solution absorption spectrum change. The NCs in micellar solution at room temperature were stable against aggregation, yet their surfaces were "reactive", in essence waiting for more reagents to be added. This realization was exploited by using a different organometallic reagent that bonded a phenyl group onto the CdSe surface. This both "capped" the NC, making the surface less reactive, and converted the particle from hydrophilic to hydrophobic. The particles exited the water droplets and settled on the bottom of the beaker. A pure dry powder of capped NCs of specific size was recovered. Working in

https://doi.org/10.1021/acsnano.1c01399
ACS Nano 2021, 15, 6192−6210

collaboration with many colleagues in Murray Hill, these capped NCs were characterized by high-resolution TEM, powder X-ray scattering, low-temperature optical hole burning spectroscopy, resonance Raman scattering, EXAFS, Auger spectroscopy, and NMR of both ^{77}Se and ^{131}Cd nuclei.[33−36]

The sequential growth idea was used to try to make potential core−shell NCs with CdSe and ZnS. If reagents for ZnS were slowly added to a CdSe micellar solution, ZnS began to grow on the CdSe surface. This process was followed in both optical absorption and luminescence. A huge increase in CdSe core luminescence was observed. These composite particles were also capped and characterized as a dry powder. The particles were poorly crystalline as they were made at room temperature, and far better methods for core−shell synthesis are known today. Nevertheless, the beneficial passivating effect of a chemically bonded, higher band gap shell was demonstrated.[37] About this time, Henglein also showed that aqueous CdS particles could be effectively capped by $Cd(OH)_2$ at high pH.[38]

After Alivisatos left to join the Berkeley chemistry faculty, further advances occurred with postdoc Moungi Bawendi who arrived in 1988. Lewis base solvents were investigated, with the hope that they would form dative bonds to surface Cd atoms and thus draw the NCs into solution. Capped CdSe powders from the inverse micelle synthesis were refluxed in 4-ethylpyridine, near 160 °C under argon. It was a surprise when this refluxing significantly sharpened the optical exciton peaks and zinc blende X-ray powder patterns. It was then realized that a higher temperature synthesis made better QDs than the room-temperature inverse micelle process. In 1989, it was found that capped micelle particles refluxed in tributylphospine TBP at 260 °C grew to *ca.* 40 Å size with excellent wurtzite structure and strong luminescence.[39,40] This was an important result. Bawendi observed that a partially empty older bottle of TBP actually gave better growth and luminescence than a new bottle. NMR analysis showed that some of the remaining TBP in the old bottle had oxidized to tributylphosphine oxide (TBPO). After this, growth was intentionally carried out in 90% TBP and 10% TBPO. Nevertheless, the growth process remained somewhat episodic. Occasionally, excellent samples with a very narrow size distribution were grown. These NCs, instead of growing at the beginning of the heating cycle, dissolved in the solution, as indicated by the disappearance of the initial yellow color. After heating for a few more hours, a deep red color slowly appeared without Rayleigh scattering, and the optical spectrum showed excellent NC exciton absorption and emission as in Figure 2B[39] and 2C.[41] It was discovered much later that traces of phosphonic acids in TBPO play a critical role in creating high-quality QD nanostructure.[42] This Bell Laboratories work on CdSe NC theory, spectroscopy, and colloidal synthesis was summarized in 1990.[43] The strong spirit of collaboration in Murray Hill made all this research possible.

At this time Brus and postdoc Karl Littau began to study silicon due to its importance in the computer/telecommunication industry. By creating a high-temperature gas-phase aerosol synthesis, they were able to observe quantum size effects and strong red luminescence in surface oxidized silicon NCs. They found that silicon does not become a direct gap due to a small size in NC form. High luminescence is created because the efficient nonradiative recombination of bulk crystalline Si, due to the long diffusion lengths of free carriers at room temperature, is prevented by confinement in NCs.[44−46]

Bawendi joined the MIT chemistry faculty and began to explore improved approaches to colloidal CdSe growth with his Ph.D. student Christopher Murray. In 1993 they found that trioctylphosphine (TOP) and trioctylphosphine oxide (TOPO) with higher boiling temperatures and toxic Me_2Cd and $(TMS)_2Se$ (or TOPSe) precursors (instead of inverse micelle powders) gave improved results. A critical insight was to limit nucleation to an initial burst. This idea was inspired by the classic work by LaMer and Dinegar in 1950, which showed that the production of a series of monodisperse lyophobic colloids depends on a temporary discrete nucleation event followed by controlled growth of the existing nuclei.[47] Murray rapidly injected cold reagent solutions into hot, near 300 °C TOP/TOPO solvent under argon, resulting in a short nucleation burst.[17] The lowering of reagent concentrations through dispersion in the large solvent volume, and the sudden temperature drop connected with introduction of room-temperature reagents, stopped further nucleation. Gently reheating allowed slow growth in size.

Solvent temperature became a powerful tool in optimizing NC growth, just as in the Ekimov glass studies. Both the average size and the NC size dispersion depend upon the growth temperature after nucleation, consistent with the surface free-energy considerations. Careful adjustment of temperature was shown to be necessary to maintain steady growth, increasing average NC size.[17] If the size distribution began to spread, the temperature necessary for slow, steady growth dropped and *vice versa*. Adjustment of the reaction temperature in response to a change in the absorption spectrum line width preserved the sharp size distribution as the sample grew.

Importantly, the slow growth kinetics necessary for high-quality NCs was supported by the capping groups (TOP/TOPO) which create a significant surface steric barrier to reaction. In comparison, slow growth kinetics in a glass matrix was achieved using the temperature dependence of the diffusion coefficient. The steady, controlled growth in hot TOP/TOPO resulted in highly monodisperse NCs and allowed size selection by extracting a sample periodically from the reaction vessel. Finally, Murray *et al.* introduced size-selective NC precipitation in mixed solvents, which resulted in a dramatic sharpening of the absorption spectra, as shown in Figure 2D. This phenomenon was also observed independently in CdS NCs by Chemseddine and Weller.[48]

All this chemical "know how" became a standard methodology for high-quality colloidal QD synthesis and enabled the controlled growth of CdS, CdSe, and CdTe (see Figure 2E). Figure 5C shows the absorption spectra of CdSe QDs with a radius of ∼1.2−11.5 nm. The frequency span of covered by the CdSe NCs is on the order of 1.2 eV. Cd_3P_2 NCs cover a larger span of 1.6 eV.[49]

SEMICONDUCTOR NCs IN SOFT CRYSTALLINE SOLIDS

NCs can be grown as inclusions in soft crystals if the diffusion coefficient of one component is sufficiently fast. In 1984, using the transverse Bridgeman method, Itoh and Kirihara grew CuCl NCs of various sizes in a NaCl host, which initially was heavily doped by Cu^+.[50] The observed blue shift of the CuCl exciton lines was explained by exciton confinement in nanometer-size crystals. Although relatively small at room temperature, the temperature-sensitive diffusion coefficient of Cu^+ in the NaCl crystal lattice enabled the growth of smaller NCs. Similar to growth in glasses, the final size distribution of the NCs is determined by the duration of the phase-separation process and is fixed at its interruption.

https://doi.org/10.1021/acsnano.1c01399
ACS Nano 2021, 15, 6192−6210

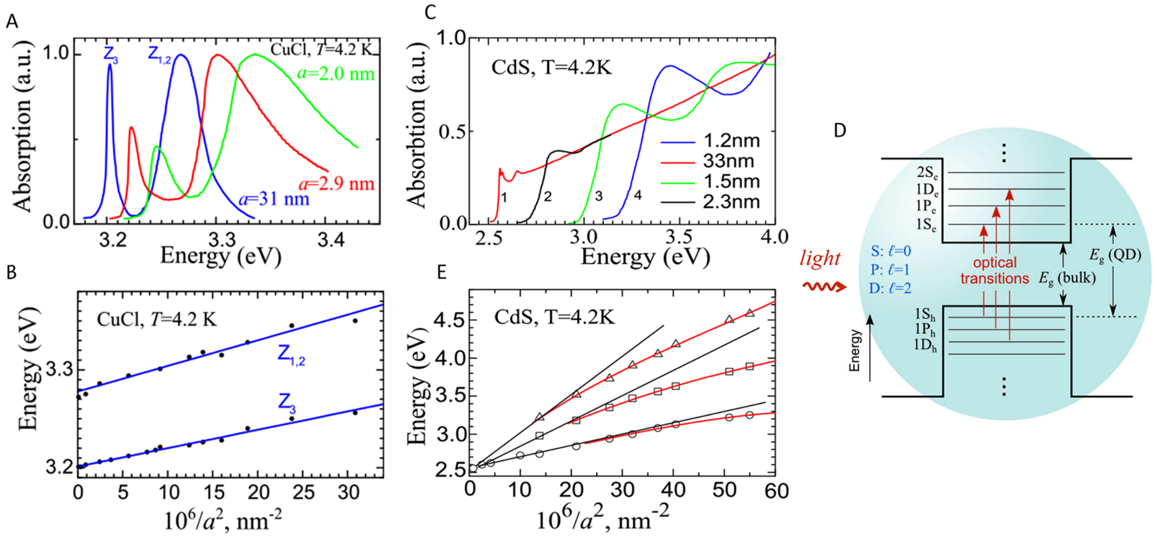

Figure 4. Size-dependent absorption spectra. (A) Absorption spectra of 2, 2.9, and 31 nm radius CuCl NCs. Adapted with permission from ref 12. Copyright 1985 Elsevier. (B) The energy dependence of the two exciton lines (Z_3 and $Z_{1,2}$) on CuCl NC radius, *a*. Adapted with permission from ref 3. Copyright 1981 Russian Academy of Science. (C) Absorption spectra of 1.2, 1.5, 2.3, and 33 nm radius CdS NCs. Adapted with permission from ref 12. Copyright 1985 Elsevier. (D) The cartoon shows schematically the structure of lowest electron and hole levels in NCs. Here we adopted level notation from atomic physics: S, P, and D for the level with angular momentum 0, 1, and 2. The arrows show the allowed transitions between these levels allowed by optical selection rules. (E) The energy dependence of the three lowest optical transitions on CdS NC radius. Adapted with permission from ref 7. Copyright 1984 Russian Academy of Science. Symbols are experimental data connected by the red lines to guide the eye. The initial slopes of the experimental dependence are shown by black straight lines.

SIZE-DEPENDENT ELECTRONIC AND OPTICAL PROPERTIES

Today it is almost impossible to imagine the initial skepticism of the solid-state community in the former Soviet Union regarding the idea that nanosize semiconductor crystals, which have only several hundred atoms, can have regular electronic and optical properties that are controlled by *just* one parameter: NC size. It was especially difficult to believe this concept because Ekimov's NCs were grown before Soviet quantum wells were created in Alferov's laboratory at the Ioffe Institute in 1984. To get the papers past the editors and peer review of Soviet journals, Ekimov and Efros decided to apply the word "microcrystal" to the nanosize semiconductor particles they were studying. Critically, the technology developed by Ekimov *et al.* for semiconductor-doped glasses in ref 1 enabled the growth of well-defined sizes and allowed researchers to establish the major size-dependent NC optical properties. The gradual change in size from very large—almost bulk (up to 1 μm in diameter)—to very small (down to 2.5 nm in diameter), which were enabled by this technique in, allowed researchers to overcome widespread skepticism that such small particles could possess regular size-dependent optical and electronic properties.

Figure 4A shows the low-temperature absorption spectra of CuCl NCs measured in three different glass samples with average NC radius a = 2.0, 2.9, and 31 nm.[12] All spectra exhibit two exciton lines connected with two valence band subbands (Z_3 and $Z_{1,2}$). One can see that the absorption spectra of the largest 31 nm radius NCs are nearly identical to those of the bulk (see Figure 1A insert) and that both exciton lines shift to the blue as size decreases. The shift of both exciton lines plotted as a function of the inverse square of the radius is shown in Figure 4B. The size dependence of the shift is linear in this scale. Extrapolation of the dependencies to very large NCs results in the energies of excitonic transitions in bulk. The observed phenomenon thus was interpreted quantum confinement of excitons in a three-dimensional (3D) NC embedded in a wide band gap oxide glass.[3] The size dependence was described by the "particle-in-a-box" equation that can be found in any handbook on quantum mechanics, assuming that the NC has a spherical shape and is surrounded by infinitely high potential barriers. This gives the following expression for the size dependence of the exciton lines:

$$\hbar\omega = E_g - E_{ex} + \frac{\hbar^2\pi^2}{2Ma^2} \quad (1)$$

where E_g and E_{ex} are the bulk energy gap and exciton binding energy of bulk CuCl. The effective mass of the exciton center of mass motion M is the only fitting parameter, determining the slope of the linear dependence in Figure 4B.

Although eq 1 qualitatively describes the exciton size shift, the effective mass M that fits the experimental slope turns out to be 40% larger than the experimentally measured value $0.2m_0$, where m_0 is the free electron mass. Usually, effective masses of wide gap semiconductors are not well-known, but this is not the case for CuCl. Precise measurements of its effective masses were conducted in the mid-1970s, motivated by the claim that CuCl is a high-temperature superconductor—a claim found to be incorrect.

The disagreement between experiment and theory brought Ekimov back to his *alma mater*, the Ioffe Institute, where he met with Alexei and Alexander Efros. Their discussions of the reasons for the disagreement clarified that eq 1 does not take into account the dispersion of sizes. The absorption coefficient of an ensemble is dominated by NCs larger than the average size.[4] This idea allowed them to describe the observed slope using the effective mass $M = (1.9 \pm 0.2)m_0$,[11] which agrees very well with the values in the literature. This meeting initiated the long lasting collaboration between Ekimov and Alexander Efros.[4]

https://doi.org/10.1021/acsnano.1c01399
ACS Nano 2021, 15, 6192−6210

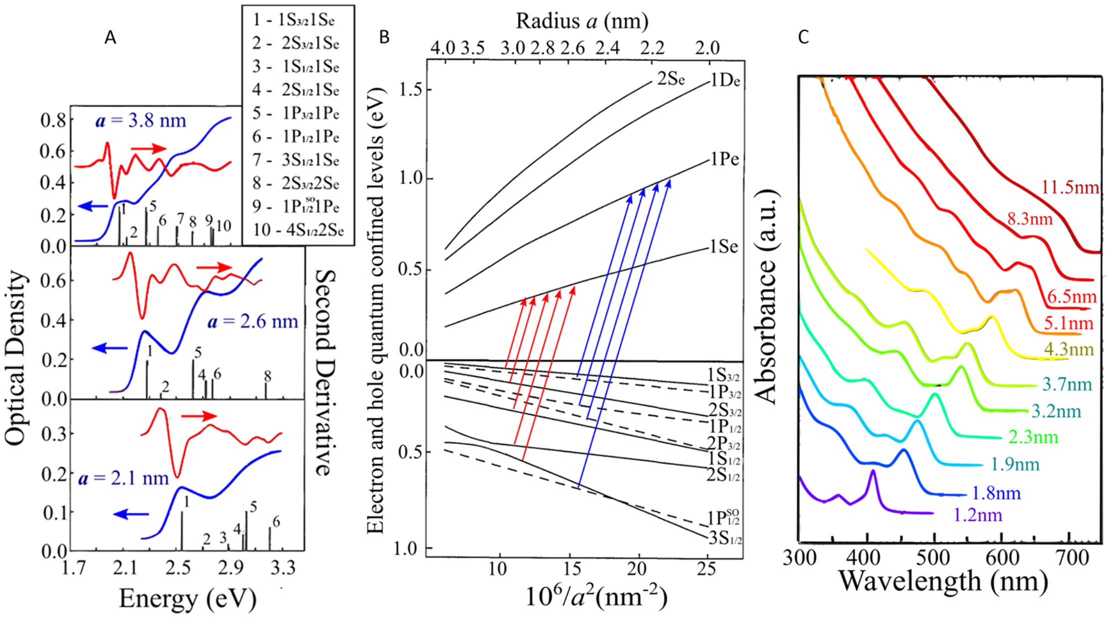

Figure 5. Size-dependent absorption spectra of CdSe NCs. (A) The absorption spectrum and its second derivation for CdSe NCs with mean radii 3.8, 2.6, and 2.1 nm. Adapted with permission from ref 16. Copyright 1993 The Optical Society. (B) The size dependence of the lowest electron and hole levels of CdSe NCs calculated within the 6-band effective mass model. Adapted with permission from ref 16. Copyright 1993 The Optical Society. The red and blue arrows show the optically allowed transitions to the 1S and 1P electron levels. The calculated position of allowed transitions and their relative intensities are indicated by the vertical lines in (A). The insert table identifies these transitions. (C) Absorption spectra of CdSe NCs with size varying from 12 to 115 Å grown in aqueous solutions. Adapted with permission from ref 17. Copyright 1993 American Chemical Society. Color of absorption lines show the real color of emission of corresponding sample.

The Coulomb interaction between the optically created electron and hole strongly affects the NC optical spectra. This interaction must always be considered because both particles—electron and hole—are confined in the same crystal volume. As a result, the optical properties depend strongly on the ratio of the NC radius, a, to the Bohr radius of the bulk exciton, a_B,[3,4] which varies in bulk semiconductors from ∼1 nm in CuCl to ∼50 nm in PbSe. A large Bohr radius results from strong carrier delocalization (small effective mass) and/or substantial screening of the Coulomb interaction. In the case $a \gg a_B$, the optical spectra of NCs are determined by the quantum confinement of the exciton center of mass motion. This case is called the "weak confinement" regime and has been carefully studied in CuCl where $a_B = 7$ Å. The "strong confinement" case is realized when $a \ll a_B$. Here the optical spectra was thought of as transitions between individual electron and hole quantum size levels, slightly decreased by the Coulomb electron–hole interaction. Detailed investigations of this case have been conducted in CdS and CdSe where $a_B = 28$ Å and $a_B = 56$ Å, respectively.

Understanding the diffusion-controlled growth of CuCl NCs made it possible to synthesize NCs of II–VI semiconductor compounds. Figure 4C shows the low-temperature absorption spectra of CdS NCs measured in four different glass samples with an average radius a = 1.2, 1.5, 2.3, and 33 nm.[11] The red curve shows the absorption spectra of very large 33 nm radius NCs. These spectra are nearly identical to the absorption spectra of bulk CdS and have a bulk energy gap equal to 2.5 eV. The fine structure at the band edge is created by the three excitons connected with the three valence subbands of this material. It is seen that a decrease in size leads to a strong shift of the absorption edge to larger energy and is accompanied by the oscillations in the higher interband absorption. The energy gap increases dramatically: up to 1 eV in the smallest NCs.

The small-size round CdS NCs are in the "strong confinement" regime. In a parabolic band approximation, each electron and hole state is characterized by angular momentum l. The energy of the corresponding levels:

$$E_{e,h}(l, n) = \frac{\hbar^2 \varphi_{l,n}^2}{2m_{e,h}a^2} \tag{2}$$

is inversely proportional to the effective mass of carriers $m_{e,h}$ and the square of the radius a, and $\phi_{l,n}$ is the n-th root of the spherical Bessel function of index l. The lowest roots are $\phi_{0,1} = \pi$, $\phi_{1,1} \approx 4.49$, $\phi_{2,1} \approx 5.76$, and $\phi_{0,2} = 2\pi$. The diagram in Figure 4E shows schematically the level structure and optically allowed transitions between electron and hole levels. Here we adopt level notation from atomic physics: S, P, and D for the levels with angular momentum 0, 1, and 2. The optical transition energies can be written:[4,5,8]

$$\hbar\omega_{l,n} = E_g + E_e(l, n) + E_h(l, n) - 1.8\frac{e^2}{\kappa a} \tag{3}$$

where κ is the semiconductor dielectric constant. The last term takes into account the electron–hole Coulomb attraction, which is calculated perturbatively.

Figure 4E shows the experimental size dependence of the band edge (empty circles) and spectral position of oscillations maxima (empty triangles and squares), for CdS at liquid helium temperatures, as a function of the inverse square of the radius. The red lines going through these data are plotted as eye guidance. The dependencies should be almost linear in $1/a^2$ scale in the parabolic approximation, as predicted by eq 3. The deviations from linear dependence are connected with the nonparabolicity of the electron energies. The initial slopes of the curves that describe the absorption spectra in very large NCs (black lines) are in good agreement with eq 3 using the electron effective mass $m_e = 0.2m_0$ known for bulk CdS. Only electron levels are resolved in the absorption spectra. The 15% dispersion of sizes was too large to resolve the hole level structures. The spacing between hole levels is small due to the large hole effective masses in CdS.

It took 9 more years for the structure of the hole levels in CdSe NCs to be revealed, which occurred when Ekimov was able to narrow the size distribution. Figure 5A shows the absorption spectrum and its second derivation for NCs with mean radii 3.8, 2.6, and 2.1 nm.[15] This observed level structure, however, cannot be described within the parabolic-band model even qualitatively. The valence band of CdSe consists of six subbands, which change both the level structure and optical selection rules.[51] The complete description of absorption also takes into account the nonparabolicity of electron spectra. Figure 5B shows the size dependence of the lowest electron and hole levels calculated within the six-band effective mass model plotted as a function of the inverse square of the radius. The red and blue arrows in Figure 5B show the optically allowed transitions to the 1S and 1P electron levels. One can see that there are no selection rules connected with the main quantum number, and transitions to the lowest electron s and p levels are allowed from many hole levels that have s and p angular symmetry.

The results of comparison of theoretical results with experiment are shown in Figure 5A. The calculated position of permissible transitions and their relative intensities are indicated by their positions, and transition intensities are in good agreement with experimental data.[16] It was later shown by Norris and Bawendi[52] that the same theory successfully describes the size-dependent absorption spectra of colloidal CdSe NCs shown in Figure 5C.

In the United States, when Brus observed the colloidal CdS NC blue shift, he was aware of the optical effects of 1D quantum confinement in thin semiconductor superlattices grown by molecular beam epitaxy. 1D confinement in superlattices was analyzed with effective mass theory in 1974.[53] In comparison, in a compact perfect NC with 3D confinement, the independent quantum energies along the three axes would simply add. A planar thin semiconductor with interfaces to higher band gap thick capping layers having essentially the same dielectric constant as the NC is especially simple, compared to NCs with real surfaces in colloids. In superlattices, the epitaxial interfaces do not introduce localized defect states, unlike the surfaces of colloidal NCs, and the electron−hole Coulomb interaction is fully screened as in the bulk crystal. Brus modeled NCs, incorporating both effective mass quantum confinement, and dielectric polarization with increased Coulomb interaction, on an equal footing.[5,8]

The fact that the electron−hole interaction is screened in the bulk crystal necessarily implies that a single charge in a NC has a significant dielectric stabilization energy. In a bulk semiconductor, the dielectric constant can be on the order of 10, and thus the Coulomb interaction between electron and hole is weaker by this factor as compared with vacuum. In a colloid, the NC dielectric constant can be a factor of 5−10 greater than that of the host liquid. This difference creates significant size-dependent polarization energies that must be considered in addition to quantum effects.[5] If a NC contains just one carrier, the electric field lines pass across the surface and terminate at infinity in the host liquid. This electrostatic problem for a spherical NC in a medium of different dielectric constant can be modeled using image charges. For a flat surface, the potential created by the image charge is shown in Figure 6A. There is a polarization force pulling the carrier to the NC center, which is the point of greatest stabilization (see Figure 6B). These electrostatic effects by themselves change the NC ionization and redox potentials, and electron affinity, as a function of size. Such dielectric polarization effects are quite general. They are important in the luminescence of Si NCs in porous silicon films,[54] in the Marcus theory of electron-transfer reactions in chemistry and biology,[55] and in luminescent carrier recombination in bulk lead-halide perovskites.[56]

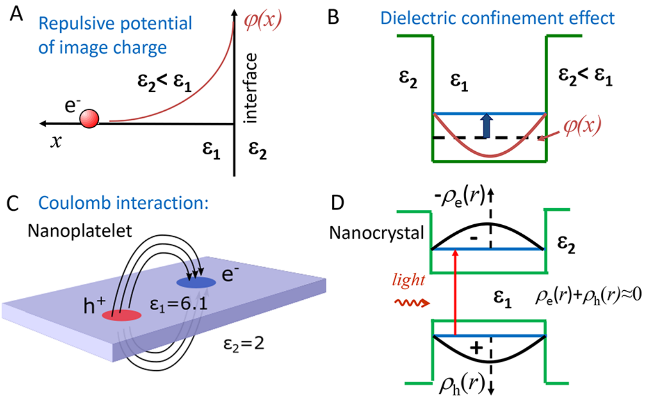

Figure 6. Effects of difference in dielectric constant and surrounding media. (A) Potential created by image charge pushes electron from the surface. (B) Cartoon that shows that the mirror force potential in a semiconductor nanostructure embedded in the media with small dielectric constant results in the shift of carrier confined level to the higher energy; this is the dielectric confinement effect. (C) The enhancement of the Coulomb interaction due to penetration of the electric field of carrier confined in nanoplatelets in the surrounding media. (D) Absence of the Coulomb enhancement in spherical NCs due to local compensation of electron and hole charge at each point of the NCs.

In contrast with a charged NC with one carrier, the electric field lines begin on the hole and terminate on the electron in an exciton of a neutral NC. The two single charge polarization fields substantially cancel with strong 3D quantum confinement (see Figure 6D). To the extent that the field lines fringe outside the NC into a lower dielectric constant of the liquid, the Coulomb interaction is stronger (less screened) than in the bulk crystal.[8] The Coulomb interaction depends upon the exact positions of the charges; the Coulomb energy can be averaged in perturbation theory only for strong quantum confinement, as shown above in eq 3. The quantum size effect increases the band gap and varies approximately as a^{-2}, while the Coulomb energy decreases the band gap and varies as a^{-1}. Thus, Coulomb energies are relatively more important in larger NCs. It is interesting to note that in 1979 Keldysh considered the Coulomb interaction inside a thin 2D dielectric layer in vacuum.[57,58] As the electron and hole move further apart, a greater fraction of the electric field fringes out into the vacuum (see Figure 6C). For large separations with respect to the dielectric thickness, the Coulomb interaction is unscreened. For close separations, the interaction is partially screened and varies as $\log(r^{-1})$, where r is the electron−hole separation.

FURTHER TECHNOLOGICAL DEVELOPMENTS

The Murray *et al.* paper[17] introduced a versatile and reproducible chemical strategy and synthesis for growing monodisperse NCs in a wide range of sizes. In contrast to NCs grown in a glass matrix, in liquid colloids, capped NCs can

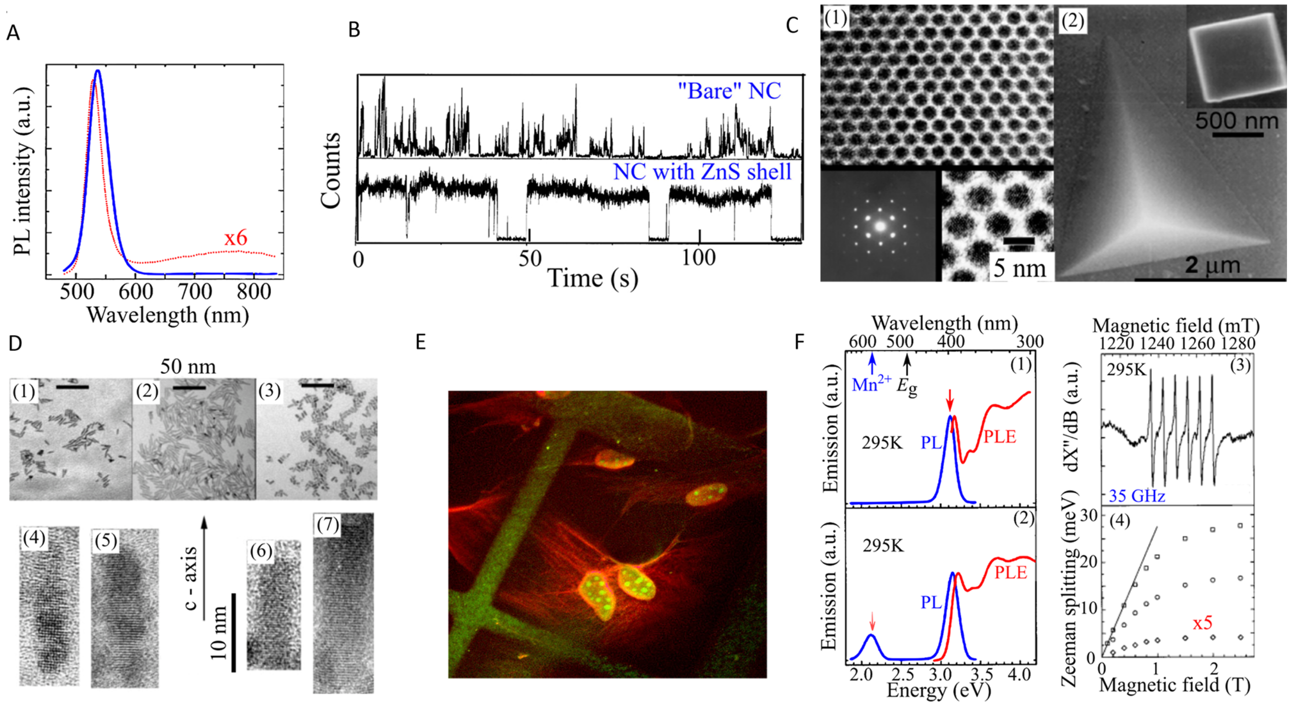

Figure 7. Technological milestones. (A) Photoluminescence (PL) of CdSe NC passivated by TOPO (dotted line) and CdSe NCs passivated by ZnS (solid line) normalized by their absorption at excitation wavelength (470 nm). Adapted with permission from ref 59. Copyright 1996 American Chemical Society. (B) Time dependence of photoluminescence intensity of a single 2.1 nm radius CdSe NCs. Adapted with permission from ref 69. Copyright 1996 Springer Nature. Excitation intensity I = 0.7 kW/cm^2, a sampling interval of 20 ms; bare NC (upper panel) and cover by seven monolayers-thick ZnS layer (lower panel). (C) (1) A $(101)_{SL}$ projection of an fcc array of 2.4 nm radius NCs with characteristic ED pattern shown in the inset. (2) TEM image of NC solid crystal made of 2.4 nm radius CdSe NCs showing the characteristic pyramidal shape. Adapted with permission from ref 70. Copyright 1995 The American Association for the Advancement of Science. (D) TEM images of different sample of nanorods. Adapted with permission from ref 75. Copyright 2000 Springer Nature. (1−3) Low-resolution of TEM images of three nanorod samples with different sizes and aspect ratios; (4−6) High-resolution TEM images of four nanorods. (E) Two-color labeling of mouse 3T3 fibroblast with green and red CdSe NCs. Adapted with permission from ref 82. Copyright 1998 The American Association for the Advancement of Science. (F) PL and photoluminescence excitation (PLE) spectra of undoped (1) and Mn-doped (2) ZnS NC, (3) fine structure electron paramagnetic resonance, and (4) magnetic field dependence of a giant Zeeman splitting of the band edge transitions measured with magnetocircular dichroism in Mn-doped ZnS NC. Adapted with permission from ref 90. Copyright 2001 American Chemical Society.

be grown and passivated in a planned sequential manner and then recovered and utilized in devices and applications for bottom-up assembly. Thousands of scientists and engineers use this chemical technology and its modifications today. We list below some important milestones.

(1) The sequential growth of designed core−shell structures, as previously described for the micelle synthesis, now using high-temperature TOP/TOPO type solvents for better crystallinity. Core−shell structures protect excitons from nonradiative recombination at the surface and thus increase the photoluminescence quantum yield.[36−38] In 1996, Hines and Guyot-Sionnest[59] demonstrated that the photoluminescence ensemble quantum yield cold be as high as 50% at room temperature in CdSe/ZnS core−shell NCs (see Figure 7A). Substantially more complex core−shell structures are grown today.[60] They are designed to satisfy additional requirements such as suppression of nonradiative Auger processes[61,62] and dislocations[63] and to have specific ligand passivation.[64,65] This subject has been substantially reviewed.[66−68]

(2) Room-temperature luminescence dynamics of individual NCs. A collaboration between MIT and Murray Hill reported the "luminescence blinking" of single CdSe/ZnS core−shell NCs under continuous illumination at room temperature (Figure 7B).[69] The observation of blinking confirms that luminescence results from coherent, single state emission by the entire NC. Blinking decreased with shell thickness, demonstrating the importance of a higher band gap shell in reducing carrier penetration to the surface. It was also realized that previous ensemble spectroscopic studies had averaged out the amazingly wide range of dynamical behavior showed by individual NCs, and this stimulated further work on improved chemical synthesis.

(3) The crystallization of a 3D periodic NC array, bound by van der Waals forces, from a supersaturated solution was reported by Murray *et al.*[70] Figure 7C shows the TEM (1) and optical images (2) of such a 6.3 nm CdSe NC "supercrystal". Periodic arrays in principle can be made from an unlimited number of man-made NCs. Many types of supercrystals with different shapes, sizes, and compositions have been grown.[71,72] The growth of binary supercrystals, that is, the ordered cocrystallization of two different NCs, has been reviewed.[73,74]

(4) Control of colloidal NC shape. Xiaogang Peng, a postdoc in the Alivisatos laboratory in Berkeley,[75] found syntheses to grow strongly elongated CdSe NCs, so-called nanorods, as shown in Figure 7D. The panels (1−3) show

https://doi.org/10.1021/acsnano.1c01399
ACS Nano 2021, 15, 6192−6210

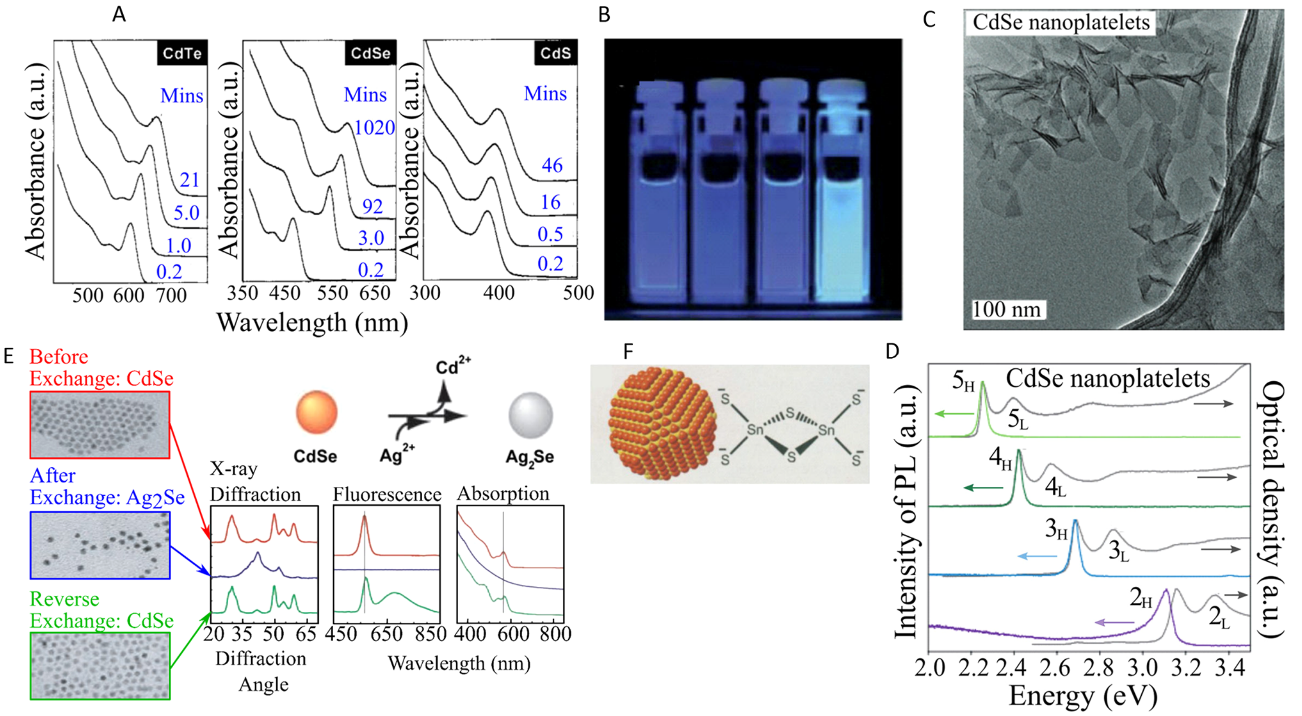

Figure 8. Technological milestones. (A) Temporal evolution of sizes and their distribution of CdTe, CdSe, and CdS NC grown using a CdO precursor. Adapted with permission from ref 96. Copyright 2001 American Chemical Society. (B) Highly efficient deep blue emitters (stared from left): 9,10-diphenylentrance, CdSe/ZnS NCs grown for 60, 40, and 20 min. All optical densities of the solution are 0.1. Adapted with permission from ref 100. Copyright 2005 Royal Society of Chemistry. (C) TEM image of five monolayer-thick CdSe nanoplatelets. Adapted with permission from ref 107. Copyright 2011 Springer Nature. (D) Absorption spectra and photoluminescence measured in two-, three-, four-, and five-monolayer-thick nanoplatelets. Adapted with permission from ref 107. Copyright 2011 Springer Nature. (E) TEM images of CdSe NCs transformed into metallic Ag_2Se NCs and then reversed back to CdSe NCs. The transformations are confirmed by X-ray diffraction, fluorescence, and absorption of corresponding samples. Adapted with permission from ref 112. Copyright 2004 The American Association for the Advancement of Science. Cartoons show schematically the cation exchange process. (F) Structure of inorganic SnS_2 ligand connected with NC surface. Adapted with permission from ref 112. Copyright 2004 The American Association for the Advancement of Science.

ensemble nanorods and panels (4−7) show the four single nanorods. Control of shape is important, due to the strong dimensionality dependence of dielectric polarization, quantum confinement, and electron correlation. For example, nanorod luminescence is linearly polarized, and the binding energy of excitons is much larger, as compared with near round QDs.[76,77] More complicated heterostructure nanorods, such as "dot-in-rods" and "nano-bar-bells", are grown today.[78] The growth of nanorod and nanorod heterostructures made of various semiconductors has been reviewed.[79,80] More complex geometrical structures, so-called tetrapods, can be grown using these approaches. There is a narrow window of reaction conditions under which CdTe nucleates in a compact zinc blende structure followed by growth of four "arms" with a wurtzite structure.[81]

(5) Nanocrystal QDs as fluorescent biological labels. In 1998, the Alivisatos group reported two color labeling and imaging, from incorporation of two different QDs, in mouse 3T3 fibroblasts *in vitro* (Figure 7E).[82] At the same time, Chan and Nie demonstrated QD imaging in cultured l HeLa cells, showing that QDs are biocompatible with living cells.[83] Subsequently frog embryos were followed throughout their growth into adult frogs using four-color QD imaging.[84] Today, control of surface chemistry on many different sizes and materials allows NC incorporation into different areas of living cells. Infrared-emitting InAs core/multishell NCs with phospholipid surface functionalization have been used in the real-time internal imaging of live mice.[85] Nanocrystal QDs are useful as optical markers because they have broad absorption spectra yet narrow emission spectra, with high brightness and photochemical stability. They can be intentionally bonded to biological molecules.[86,87] In neurons, the NC submillisecond responsiveness due to a relatively short radiative decay time, and a two-photon cross section larger than that of fluorescent dyes, enable their use in monitoring of electrical activity.[88] Also, note that in 1989, Brus, Winge and collaborators discovered naturally occurring quantum confined CdS NCs, capped with cysteine rich peptides, in yeasts.[89]

(6) Synthesis of intentionally doped NCs. Controlled doping was reported by Norris *et al.*,[90] in which high-quality ZnSe NCs were doped with Mn. Previously, it had been suspected that this would be essentially impossible due to spontaneous NC lattice self-purification. Figure 7F shows the spectra of undoped (1) and Mn doped (2) ZnSe NCs and clearly shows the Mn emission line in the doped sample. Figure 7F shows the electron paramagnetic resonance fine structure resulting from substitutional internal Mn (3) and the giant magneto circular dichroism due to the Mn effective magnetic field (4). Various doping mechanisms and syntheses have been reviewed.[91−94]

(7) Safer reagents. Peng, working with his own group in the early 2000s, explored benign reagents. Some organometallic precursors, such as $Cd(CH_3)_2$ used in the earlier

https://doi.org/10.1021/acsnano.1c01399
ACS Nano 2021, 15, 6192−6210

Murray Hill and MIT work, are toxic, pyrophoric, expensive, and unstable at room temperature. Also, gases such as H_2Se are dangerous, as shown by the accident that sent Brus to the hospital in 1986. Peng and Peng[95] showed that $Cd(CH_3)_2$ could be replaced by more benign CdO while still growing high-quality CdTe, CdSe, and CdS NCs of different sizes with shape control, as shown in Figure 8A.[96] Peng moreover grew high-quality InP NCs, using indium acetate ($In(Ac)_3$) and tris(trimethylsilyl)phosphine ($P(TMS)_3$) precursors and octadecene as a noncoordinating solvent.[97] The III−V QDs are generally more difficult to make than II−VI NCs as they are more covalent. Today the use of benign precursors is standard.[98,99]

(8) Graded alloy interfaces and structures. Strain and localized defect states which degrade luminescence can occur at an abrupt CdSe/ZnS core−shell interface, due to the 7% lattice mismatch. In 2005 Eunjoo Jang, working in the Samsung Laboratories in Korea, discovered that an interdiffused interface could be grown at 300 C using less reactive ZnS precursors, compared with a more abrupt interface grown near 160 °C with more reactive precursors.[100] She was able to grow blue-emitting QDs with significantly improved quantum yield; see Figure 8B. Today the ideas of a more gradual, graded interface, and different alloy compositions for core and shell, are widely adopted.[101,102] Besides reducing defects and blinking, a gradual interfacial potential step reduces nonradiative Auger recombination.[103] Owen and his group have explored the connection between precursor reactivity and QD size and properties. They created an extensive library of chalcogenourea reagents showing a wide range of reactivities.[104]

(9) Quasi-two-dimensional colloidal platelets. CdSe nanoribbons with 1.4 nm thickness were reported,[105] and later Ithurria and Dubertret demonstrated a controlled growth of two-dimensional CdSe structures termed nanoplatelets.[106] The TEM image of five monolayer-thick CdSe nanoplatelets is shown in Figure 8C. With similar growing techniques, CdS and CdTe platelets with thicknesses varying from one to seven monolayers have been made.[107] These structures have electronic properties similar to freestanding quantum wells, with band edge absorption showing light and heavy hole transitions, and strong emission from the heavy hole exciton, as one can see in Figure 8D.[107] Due to enhancement of the exciton binding energy and a giant oscillator strength, these platelets can be especially fast luminophors.[107] More complex core−shell,[108] core−crown,[109] and epitaxial multishell nanoplatelets have been reported recently.[110]

(10) NC modification by cation exchange. Cd replacement by Hg with unchanged anion lattice was observed in the growth of CdS/HgS/CdS multishell structures.[111] Later Alivisatos and students reversibly transformed CdSe NCs into metallic Ag_2Se NCs and then back to CdSe, as shown in Figure 8E.[112,113] This chemistry was also used to make geometrically complex PbSe/CdSe core−shell NCs,[114] to attach NCs to a honeycomb superlattice,[115] and to perform doping.[116,117] This chemistry is amazingly versatile[118] as described in a recent review.[119]

(11) Inorganic ligands to increase electrical coupling between NCs. In electrical transport of dense NC films in prototype solar cells, LEDs, and photodetectors, good electrical coupling between NCs is critical.[120,121] For this purpose, small inorganic ligands, such as SnS_2 shown in Figure 8F, have proven to be far better than the larger organic Lewis base-type ligands required in the synthesis. These organic capping ligands can be subsequently exchanged for the inorganic ligands, increasing the electrical overlap integral between NCs, and thus the carrier mobility of the film. Recently this approach was extended to metal-halide ligands which significantly improve the operation characteristics of PbS NC prototype photovoltaic cells[122] and LEDs.[123]

IMPORTANT CLASSES OF NCs

Practically all known inorganic semiconductors have been prepared in NC form. We now describe several important classes.

(1) Pb chalcogenides NCs. Brus[10] and Nozik *et al.*[124] made room-temperature PbS colloids, however without precise control of size. Borrelli and Smith[125] in the Corning Glass company reported the size dependence of PbSe and PbS NC optical properties, measured in a glass host. Accurate modeling requires the Kang and Wise four-band effective mass model which takes into account the nonparabolicity of the conduction and valence bands.[126] More recently, Murray and collaborators invented a synthesis that controls composition, size, and shape.[127] Today, conductive NC films are explored in prototype solar cells,[128,129] due to the match of their absorption to the solar spectra, and in room-temperature infrared photodetectors.[130,131]

(2) Silicon NCs. Both Si NCs grown near 900 °C in an aerosol[44−46,132] and nanostructured porous Si films created by HF electrochemical etching exhibit a high photoluminescence quantum yield. This excited hope that some form of commercially useful optical active Si might be created. In a formal sense, spatial confinement of carriers mixes the X and Γ critical points of the Brillouin zone, creating direct (dipole allowed) band edge transitions which are forbidden in the indirect gap bulk. However, experiments show this mixing is extremely weak and essentially Si remains indirect gap in NC form.[44,133] More recently, hexagonal SiGe alloy nanowires have shown a more significant direct gap character.[134]

(3) InP NCs. Micic *et al.*[135] made InP NCs in 1994. The synthesis was significantly improved by Peng *et al.*, as discussed earlier, and by Li and Reiss.[136] As InP does not contain a toxic heavy metal, Jang and her colleagues in the Samsung laboratories intensively developed the synthesis of high-quality InP-based core−shell NCs as red and green emitters in liquid crystal displays. In 2019, they further reported InP/ZnSe/ZnS core−double shell QDs with nearly perfect performance when excited electrically (rather than optically) in prototype LEDs. Synthesis required extreme reagent purification and intermediate HF etching of colloidal InP cores to remove oxide impurities. This was followed by controlled ZnS growth at 340 °C and subsequent exchange of surface ligands. These NCs could be used in commercial QD LED displays.[63]

(4) Gapless HgTe NCs. 3D confinement opens the optical gap in HgTe NCs to near 1 eV with decreasing size. HgTe NCs were grown in aqueous solution by Rogach *et al.*[137] This synthesis has been improved dramatically, allowing

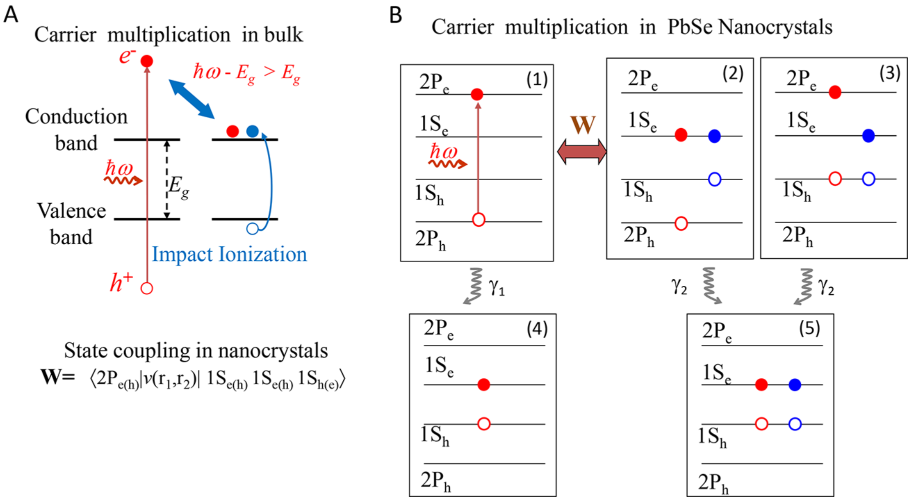

Figure 9. Carrier multiplications or impact ionization. (A) Cartoon shows this process in bulk. Optically excited electron with excess energy $\hbar\omega - E_g > E_g$ can create the second electron in the conduction band *via* impact ionization of the valence band. Adapted with permission from ref 166. Copyright 2013 American Chemical Society. This process is inverse to the direct Auger recombination, the process during which the recombining electron−hole pair transfers its annihilation energy to the second electron. (B) Cartoon showing carrier multiplication in PbSe NCs: (1) The energetic threshold of the carrier multiplication in PbSe NC which is the $2P_e2P_h$ transitions. (2 and 3) Electron (hole) in $2P_{e(h)}$ states could create thrions consisting of two electrons (holes) and one hole (electron) on the lowest confined $1S_{e(h)}$ levels correspondingly due to strong coupling between electron and trion states described by the matrix element $W = \langle 2P_{e(h)}|v(r_1,r_2)|1S_{e(h)}1S_{e(h)}1S_{h(e)}\rangle$. Adapted with permission from ref 164. Copyright 2006 American Chemical Society. The optically excited pair in (1) can thermalize to a single exciton state shown in (4) with themalization rate γ_1. However, this thermalization is suppressed in NCs due to their discrete spectra resulting in phonon bottleneck.[137] The multiexciton states in (2) and (3) are thermalized with a rate γ_2 to the ground two electron−hole pair state shown in (5).

use of NC films as prototype infrared detectors in the short- (1.5−2.5 μm), mid- (3−5 μm), and long-wave (8−12 μm) ranges.[138] The size and shape homogeneity of HgTe NC films is now so high that they show band electrical transport rather than hopping transport.[139]

(5) $CsPbX_3$ (X = I, Br, Cl) perovskite NCs. Perovskites differ from earlier II−VI, III−V, and IX semiconductors in that they show nearly ionic bonding. Even without surface passivation or core−shell structure, NCs show both a high photoluminescence quantum yield and very narrow emission lines at room temperature. Photoluminescence covers the entire optical range from the infrared to the far ultraviolet, with different sizes and compositions.[140] High luminescence is caused by a short radiative lifetime and the apparent absence of surface trap states. At room temperature, the exciton radiative lifetime is on the order of several ns,[141] perhaps 20 times shorter than that of CdSe NCs. These NCs might be used in possible LEDs, lasers, and in other electro-optical application, especially in the difficult green and blue spectral regions.[142] However, a serious problem for practical use is the presence of toxic Pb in a material that easily dissolves in water.

INTERMEDIATE EFFECTS AND THE MOLECULAR LIMIT

NCs represent a physical regime intermediate between molecules and the bulk solid state. Aspects of their behavior can sometimes be more transparent from a molecular perspective and sometimes from a solid state perspective. Separate chemical and physical approaches can yield the same result, for example, the parabolic effective mass model in momentum space is equivalent to the tight binding molecular orbital model for band development in real space.[40] Smaller NCs showing strong confinement with discrete energy levels are essentially large molecules and are well understood within molecular chemistry. Density functional theory structural calculations can reveal properties not shown by effective mass models, especially with respect to surface bonding and structure. In the strong confinement limit, the spatial patterns of the electron and hole wave functions are determined by atomic positions and not by their mutual Coulomb attraction. This HOMO−LUMO state is essentially a molecular excited electronic state. Nevertheless, it is labeled an exciton for historical reasons. In comparison, excitons in larger NCs of various shapes, and with crystalline interiors, have a clear parentage in solid-state physics and can be effectively analyzed from a band structure perspective. There has been significant theoretical effort using a number of different approaches.[143−152]

One interesting effect in the intermediate regime is the "non-local Coulomb" attraction between electron and hole, as described previously. The mutual force felt by electron and hole depends upon their exact positions within the NC, in addition to the distance between them, as shown in Figure 3D. Another effect is the "intermediate" confinement regime, realized if the hole effective mass is much larger than the electron mass. In this case, there is a range of sizes wherein the confinement energy of the electron, E_e, is much larger than the energy of the shielded Coulomb interaction $e^2/\kappa a$, which in turn is much larger than the hole confinement energy E_h. The hole energy spectra and selection rules are strongly modified because the holes move in the adiabatic potential created by strongly confined electrons.[4] Ekimov *et al.* realized all three confinement regimes in different semiconductors:[3,7,11,16] "strong" in CdS and CdSe NCs, "intermediate" in CdS and CuBr NCs, and "weak" in CuCl and CuBr NCs. Today this concept is also used for describing the optical properties of various QDs, nanowires, nanorods, and nanoplatelets.

The 1990 Bawendi *et al.*[41] and 1994 Nirmal *et al.*[153] papers on CdSe NC resonantly excited photoluminescence report an emission vibrational structure with a small Stokes shift relative to the lowest exciton absorption band in Figure 2C. A zero phonon line and a few weak longitudinal optical phonon satellites are observed. NC luminescence colors in optical displays are vivid because this electron-vibration coupling is not strong. In comparison, stronger electron-vibration coupling is nearly universal in molecular spectroscopy. Also, the photoluminescence lifetime at low temperatures is extremely long—on the order of 1000 ns. This results from the electronic fine structure of the degenerate band-edge exciton, consisting of optically allowed and optically forbidden states with a splitting on the order of kT at room temperature. Similarly, in molecular spectroscopy, degenerate (either spin or orbital) electronic states often show fine structure. This result led to further development of the dark/bright exciton model in NCs,[154−156] and somewhat later in nanowires, nanorods, and nanoplatelets.

In 1987, Schmitt-Rink and Chemla modeled potential applications involving optical nonlinear spectroscopy and lineshapes in NCs.[157] They demonstrated that a photoexcited electron−hole pair has a reduced interaction with polar optical phonons due to the almost complete compensation of electron and hole charge distributions at each point in a spherical NCs, despite of the fact that the polar phonon interaction with individual carriers can be significant in a small NC (see Figure 6D). This reduced coupling was observed in the CdSe photoluminescence experiments described above. This effect is analogous to the near cancelation of static dielectric polarization fields in a neutral exciton, as described earlier.

The observation of very efficient Auger recombination[158] and photostimulated Auger ionization[159] in NCs was unexpected. In the latter phenomenon, a photoexcited electron−hole pair transfers its energy to a pre-existing extra carrier. The NC ionizes and photoluminescence is quenched. Such Auger processes are suppressed in bulk wide gap semiconductors like CdSe or CdS.[160] Both NC phenomena were discovered in the study of the CdS QD photoluminescence intensity in glass. The dependence of the degradation rate on the intensity and frequency of the exciting light demonstrated Auger stimulated ionization, where two electron−hole pairs were excited simultaneously, along with the complete quenching of photoluminescence. This phenomenon can also cause intermittency of luminescence intensity (“blinking”), in single QDs under continuous irradiation, as shown in Figure 7B.[69] In single molecules blinking, due to either photoionization or population trapping in a long-lived metastable excited state, also occurs commonly. Today, efficient nonradiative Auger recombination is recognized as the primary reason for the progressive decrease in photoluminescence quantum efficiency in prototype LEDs and for the increase in the stimulated emission threshold in prototype lasers based on quantum well structures. Studies of the size dependence of Auger recombination rate have been reported and reviewed.[161,162]

Carrier multiplication or impact ionization—the creation of two electrons and one hole from one high energy electron—is inverse to the Auger process (see Figure 9A). Carrier multiplication could increase the efficiency of NC based solar cells, because the extra energy of a hot photoexcited electron could create a second electron−hole pair instead of heating the sample. As discussed above it was shown theoretically and experimentally that the rate of direct Auger processes, during which two electrons and one hole create one excited electron, is strongly enhanced in NCs. Arthur Nozik suggested that the inverse Auger process should also be enhanced because both are controlled by the same transition matrix element[163] related to the multielectron Coulomb interaction $v(r_1,r_2)$. In addition, carrier thermalization is suppressed due to the discrete character of QD quantum levels creating a partial phonon bottleneck. In PbSe QDs (see Figure 9B), this transition takes place between the $|2P_{e(h)}\rangle$ electron(hole) level and the $|1S_{e(h)}1S_{e(h)}1S_{h(e)}\rangle$ two electron (hole) and one hole(electron) trion state, in which the degenerate 1S electrons (holes) have opposite spins and is written as $\langle 2P_{e(h)}|v(r_1,r_2)|1S_{e(h)}1S_{e(h)}1S_{h(e)}\rangle$.[164] In this connection, stochastic Fermi golden rule calculations show that the carrier multiplication rate is strongly influenced by the density of final states as well as the matrix element.[165−167] Carrier multiplication was observed in the bleach of band edge absorption of PbSe QDs by Schaller and Klimov.[128] It has also been reported in other QDs, and extra carriers created by a single photon have been directly observed in the electrical transport of prototype solar cells.[168] However, to date, the reported overall increases in prototype QD solar cell efficiencies from carrier multiplication have been small.[169] At a fundamental level, strong carrier multiplication and exciton binding are both consequences of increased electron−electron repulsion and correlation in nanostructures, as compared with bulk 3D solids.[170]

As previously discussed, a small dielectric constant in the surrounding media increases the strength of the electron−hole Coulomb interaction resulting in large exciton binding energies, up to 0.4 eV, in nanorods, nanowires, and nanoplatelets.[76,171−173] At optical frequencies, the difference between the dielectric constants of a nanostructure and the surrounding media also creates dielectric confinement, similar to that described for static electric fields described earlier. This confinement can strongly influence optical absorption and polarization properties. For larger nanostructures, the strength of external light coupling to internal excitons depends strongly on the electromagnetic field direction relative the nanostructure surface. If the electric field of an external photon is parallel to the nanostructure surface, its magnitude inside the nanostructure is unchanged. However, if the field is perpendicular, then its magnitude inside is reduced by a ratio of the external to internal dielectric constants. When this occurs, optical polarization in the nanostructure coherently reacts back upon the nearby external optical field, creating regions (hot spots) of higher and lower intensity. This phenomenon leads to polarization memory effects in anisotropic nanostructures[174,175] and to the SERS enhanced Raman effect in Ag metallic nanostructures. On macroscopic surfaces, these effects create refraction and reflection of incident light beams. In comparison, individual molecules typically are within the point dipole limit in their coupling to an optical field, and thus dielectric confinement does not occur.

In 1962, Rashba[176] predicted that coherent motion of weakly bound excitons in a bulk 3D semiconductor could create a giant oscillator strength state, with drastic shorting of the observed lifetime. In bulk, this phenomenon has been observed for excitons bound to shallow impurities and was also observed in CuCl NCs that show a radiative decay time ~100 ps at helium temperature.[177] More recently, coherent shortening of the radiative decay time has also been observed in large perovskite $CsPbX_3$ NCs.[178]

INTO THE FUTURE

NC research and development continues with strong momentum. This is a true interdisciplinary field, at the mutual junction of chemistry, physics, and materials science. One might say that the development of NC materials science over the last

20 years resembles the development of bulk semiconductor technology in the mid-20th century. Today hundreds of scientists and engineers are working on improved NC designs, synthesis, and prototype devices.

The field is not yet mature. Just 5 years ago, the lead halide perovskite QDs were discovered. They show ease of synthesis, especially strong luminescence, an optically active lowest fine structure component, an apparent absence of surface states, and very high two-photon cross sections. If the issue of toxic Pb can be controlled, then these outstanding properties may have commercial application.

Our review documents how improved chemical synthesis has driven much of the progress of the last 20 years. Synthesis and encapsulation will remain critically important. NC nucleation and surface growth need to be understood at the molecular level. The NC field will prosper and will evolve in unexpected directions, when essentially ideal inexpensive NCs of all types of designed structure are widely available. This is an opportunity for the chemistry community.

As previously mentioned, nearly ideal core—double shell InP NCs for electroluminescence were reported in 2019. A systematic and persistent synthetic effort has also created nearly perfect photoluminescence properties in CdSe-based core—shell NCs, with quantum yields of 80—95% at room temperature.[179] The use of II—VI alloy compositions has lowered the Cd content in some structures to an acceptable level for commercial use. CdSe-based QDs are used in some TVs and displays, in addition to the InP QDs pioneered by Samsung. Within the past 2 years, Osram has begun to use CdSe-based luminescing QDs in GaN LED chips for area (*i.e.*, ceiling) lighting, creating white light of variable designed properties.

It is notoriously difficult to make predictions about future technology. Our crystal ball is cloudy. Nevertheless, we offer a few thoughts: The invention of the blue GaN LED for solid-state lighting was epochal, improving the quality of life worldwide. The combination of this LED with luminescing QDs (excited by down conversion of blue light) is a powerful technology. Such devices are energy efficient and inexpensive and can be designed to emit either pure colors or broad band white light of various hues. They work well both on a macroscopic scale, as in the Osram area lighting white LEDs, and on a microscopic scale, as in micro-LEDs which emit pure colors as single pixels in displays.[180] The use of these devices is likely to continue expanding. It is always difficult to replace an existing mature technology, but this seems to be happening in displays and possibly lighting.

A huge effort has and is being invested in creating solution processable and flexible NC-based electronic materials, which hopefully would be inexpensive and commercially useful. Controlled colloidal NC assemblies and materials for flexible electronics,[181] quantum information science,[182] optically pumped lasers,[183] and many other possibilities mentioned in the text are all being pursued. These are discussed more deeply in the references. Their success depends largely on continued chemical progress in NC quality and assembly processing. These technological developments have shown significant progress in the past decade.

AUTHOR INFORMATION

Corresponding Authors

Louis E. Brus — *Department of Chemistry, Columbia University, New York 10027, United States*; orcid.org/0000-0002-5337-5776; Email: leb26@columbia.edu

Alexander L. Efros — *Center for Computational Material Science, Naval Research Laboratory, Washington, DC 20375, United States*; orcid.org/0000-0003-1938-553X; Email: sasha.efros@nrl.navy.mil

Complete contact information is available at: https://pubs.acs.org/10.1021/acsnano.1c01399

Notes

The authors declare no competing financial interest.

ACKNOWLEDGMENTS

The authors would like to thank T. Harris, A. I. Ekimov, M. Steigerwald, D. Norris, C. Murray, H. Kaplan, V. Klimov, M. Kovalenko, D. Talapin, U. Banin, D. Vanmaekelbergh, S. Erwin, J. Owen, J. Yardley, and E. Jung for their valuable comments and suggestions and A. Chandrashekar and R. Vaxenburg for assistance with manuscript preparation. Al.L.E. acknowledges support from the Office of Naval Research through the Naval Research Laboratory's Basic Research Program. L.E.B. acknowledges support from the Kavli Foundation, the Keck Foundation, the Department of Energy, and the National Science Foundation.

VOCABULARY

Exciton, electron—hole pair bound by the Coulomb attraction; **semiconductor**, extended solid with a nonconductive gap in the band structure; **nanocrystal**, a large molecule in which the core atoms exhibit the crystal structure of the corresponding bulk compound; **quantum size effect**, energy increase of an electrical carrier due to confinement in a small crystal volume; **quantum dot**, nanocrystal characterized by a 3D confinement potential for carriers resulting in a discrete energy spectrum; **light-emitting diode**, a device which emits light as a result of recombination of electrons and holes electrically injected in two separate contacts

REFERENCES

(1) Ekimov, A. I.; Onushchenko, A. A.; Tsekhomski, V. A. Exciton Absorption by Copper Chloride Crystal in Glassy Matrix. *Fiz. Khim. Stekla* **1980**, *6*, 511—512.

(2) Golubkov, V. V.; Ekimov, A. I.; Onushchenko, A. A.; Tsekhomski, V. A. Kinetics of CuCl Microcrystals Growth in a Glass Matrix. *Fiz. Khim. Stekla* **1981**, *7*, 397—401;Translated to English in *Sov. Phys. Chem. Glass* **1982**, *7*, 265—269.

(3) Ekimov, A. I.; Onushchenko, A. A. Quantum Size Effect in Three-Dimensional Microscopic Semiconductor Crystals. *JETP Lett.* **1981**, *34*, 345—349.

(4) Efros, Al. L.; Efros, A. L. Interband Absorption of Light in Semiconductor Sphere. *Sov. Phys. Semicond.* **1982**, *16*, 772—775.

(5) Brus, L. E. A Simple Model for the Ionization Potential, Electron Affinity, and Aqueous Redox Potentials of Small Semiconductor Crystallites. *J. Chem. Phys.* **1983**, *79*, 5566—5571.

(6) Rossetti, R.; Nakahara, S.; Brus, L. E. Quantum Size Effects in the Redox Potentials, Resonance Raman Spectra, and Electronic Spectra of CdS Crystallites in Aqueous Solution. *J. Chem. Phys.* **1983**, *79*, 1086—1088.

(7) Ekimov, A. I.; Onushchenko, A. A. Size Quantization of the Electron Energy Spectrum in Semiconductor Microcrystals. *JETP Lett.* **1984**, *40*, 1136—1139.

(8) Brus, L. E. Electron-Electron and Electron-Hole Interactions in Small Semiconductor Crystallites: The Size Dependence of the Lowest Excited Electronic State. *J. Chem. Phys.* **1984**, *80*, 4403—4409.

(9) Rossetti, R.; Hull, R.; Gibson, J. M.; Brus, L. E. Excited Electronic States and Optical Spectra of ZnS and CdS Crystallites in the 15 to 50 Angstrom Size Range: Evolution from Molecular to Bulk Semiconducting Properties. *J. Chem. Phys.* **1985**, *82*, 552—559.

(10) Rossetti, R.; Hull, R.; Gibson, J. M.; Brus, L. E. Hybrid Electronic Properties between the Molecular and Solid State Limits: Lead Sulfide and Silver Halide Crystallites. *J. Chem. Phys.* **1985**, *83*, 1406−1410.

(11) Ekimov, A. I.; Onushchenko, A. A.; Plukhin, A. G.; Efros, Al. L. Size Quantization of Excitons and Determination of the Parameters of Their Energy Spectrum in CuCl. *Sov. Phys. JETP* **1985**, *61*, 891−897.

(12) Ekimov, A. I.; Efros, Al. L.; Onushchenko, A. A. Quantum Size Effect in Semiconductor Microcrystals. *Solid State Commun.* **1985**, *56*, 921−924.

(13) Ekimov, A. I.; Onushchenko, A. A.; Raikh, M. E.; Efros, Al. L. Size Quantization of Excitons in Microcrystals with Large Longitudinal - Transverse Splitting. *Sov. Phys. JETP* **1986**, *63*, 1054−1060.

(14) Chestnoy, N.; Hull, R.; Brus, L. E. Higher Excited Electronic States in Clusters of ZnSe, CdSe, and ZnS: Spin-Orbit, Vibronic, and Relaxation Phenomena. *J. Chem. Phys.* **1986**, *85*, 2237−2242.

(15) Brus, L. E. Zero-Dimensional "Excitons" in Semiconductor Clusters. *IEEE J. Quantum Electron.* **1986**, *22*, 1909−1914.

(16) Ekimov, A. I.; Kudryavtsev, I. A.; Efros, Al. L.; Yazeva, T. V.; Hache, F.; Schanne-Klein, M. C.; Rodina, A. V.; Ricard, D.; Flytzanis, C. Absorption and Intensity-Dependent Photoluminescence Measurements on CdSe Quantum Dots: Assignment of the First Electronic Transitions. *J. Opt. Soc. Am. B* **1993**, *10*, 100−107.

(17) Murray, C. B.; Norris, D. J.; Bawendi, M. G. Synthesis and Characterization of Nearly Monodisperse CdE (E = S, Se, Te) Semiconductor Nanocrystallites. *J. Am. Chem. Soc.* **1993**, *115*, 8706−8715.

(18) Kovalenko, M. V.; Manna, L.; Cabot, A.; Hens, Z.; Talapin, D. V.; Kagan, C. R.; Klimov, V. I.; Rogach, A. L.; Reiss, P.; Milliron, D. J.; Guyot-Sionnnest, P.; Konstantatos, G.; Parak, W. J.; Hyeon, T.; Korgel, B. A.; Murray, C. B.; Heiss, W. Prospects of Nanoscience with Nanocrystals. *ACS Nano* **2015**, *9*, 1012−1057.

(19) Bányai, L.; Koch, S. W. Semiconductor Quantum Dots. In *World Scientific Series on Atomic, Molecular and Optical Physics*; World Scientific: Singapore, 1993; Vol. 2.

(20) Woggon, U. *Optical Properties of Semiconductor Quantum Dots*. Springer: Berlin, 1997.

(21) Gaponenko, S. V. *Optical Properties of Semiconductor Nanocrystals*; Cambridge University Press: Cambridge, 1998.

(22) The Spectroscopy of Isolated and Assembled Semiconductor Nanocrystals. In Special Issue of the *J. Luminesc.* 1996, *70*, 1−484; Brus, L. E., Efros, Al. L., Itoh, T., Eds.

(23) *Semiconductor Nanocrystals: From Basic Principles to Device Applications*; Efros, Al. L., Lockwood, D. J., Tsybeskbov, L., Eds.; Kluwer Academic: New York, 2003.

(24) *Nanocrystal Quantum Dots*, 2nd ed.; Klimov, V. I., Ed.; CRC Press, Taylor&Francis Group: Boca Raton, FL, 2010.

(25) Lifshitz, I. M.; Slezov, V. V. Kinetics of Diffusive Decomposition of Supersaturated Solid Solutions. *Sov. Phys. JETP* **1959**, *8*, 331−339.

(26) Mau, A. W.-H.; Huang, C.-B.; Kakuta, N.; Bard, A. J.; Campion, A.; Fox, M. A.; White, J. M.; Webber, S. E. H_2 Photoproduction by Nafion/CdS/Pt Films in H_20/S_2 Solutions. *J. Am. Chem. Soc.* **1984**, *106*, 6537−6542.

(27) Tricot, Y.-M.; Emeren, A.; Fendler, J. H. *In Situ* Generation of Catalyst-Coated CdS Particles in Polymerized and Unpolymerized Surfactant Vesicles and Their Utilization for Efficient Visible-Light-Induced Hydrogen Production. *J. Phys. Chem.* **1985**, *89*, 4721−4726.

(28) Gratzel, M.; Moser, J. Multielectron Storage and Hydrogen Generation with Colloidal Semiconductors. *Proc. Natl. Acad. Sci. U. S. A.* **1983**, *80*, 3129−3132.

(29) Henglein, A. Photochemistry of Colloidal Cadmium Sulfide. 2. Effects of Adsorbed Methyl Viologen and of Colloidal Platinum. *J. Phys. Chem.* **1982**, *86*, 2291−2293.

(30) Fojtik, A.; Weller, H.; Koch, U.; Henglein, A. Photo-Chemistry of Colloidal Metal Sulfides 8. Photo-Physics of Extremely Small CdS Particles: Q-State CdS and Magic Agglomeration Numbers. *Ber. Bunsenges. Phys. Chem.* **1984**, *88*, 969−977.

(31) Koch, U.; Fojtik, A.; Weller, H.; Henglein, A. Photochemistry of Semiconductor Colloids. Preparation of Extremely Small ZnO Particles, Fluorescence Phenomena and Size Quantization Effect. *Chem. Phys. Lett.* **1985**, *122*, 507−510.

(32) Brus, L. E. Electronic Wave Functions in Semiconductor Clusters: Experiment and Theory. *J. Phys. Chem.* **1986**, *90*, 2555−2560.

(33) Alivisatos, A. P.; Harris, A. L.; Levinos, N. J.; Steigerwald, M. L.; Brus, L. E. Electronic States of Semiconductor Clusters: Homogeneous and Inhomogeneous Broadening of the Optical Spectrum. *J. Chem. Phys.* **1988**, *89*, 4001−4011.

(34) Alivisatos, A. P.; Harris, T. D.; Carroll, P. J.; Steigerwald, M. L.; Brus, L. E. Electron-Vibration Coupling in Semiconductor Clusters Studied by Resonance Raman Spectroscopy. *J. Chem. Phys.* **1989**, *90*, 3463−3468.

(35) Marcus, M. A.; Flood, W.; Stiegerwald, M.; Brus, L.; Bawendi, M. Structure of Capped CdSe Clusters by EXAFS. *J. Phys. Chem.* **1991**, *95*, 1572−1576.

(36) Steigerwald, M. L.; Alivisatos, A. P.; Gibson, J. M.; Harris, T. D.; Kortan, R.; Muller, A. J.; Thayer, A. M.; Duncan, T. M.; Douglass, D. C.; Brus, L. E. Surface Derivatization and Isolation of Semiconductor Cluster Molecules. *J. Am. Chem. Soc.* **1988**, *110*, 3046−3050.

(37) Kortan, A. R.; Hull, R.; Opila, R. L.; Bawendi, M. G.; Steigerwald, M. L.; Carroll, P. J.; Brus, L. E. Nucleation and Growth of CdSe on ZnS Quantum Crystallite Seeds, and *Vice Versa*, in Inverse Micelle Media. *J. Am. Chem. Soc.* **1990**, *112*, 1327−1332.

(38) Spanhel, L.; Haase, M.; Weller, H.; Henglein, A. Photochemistry of Colloidal Semiconductors. 20. Surface Modification and Stability of Strong Luminescing CdS Particles. *J. Am. Chem. Soc.* **1987**, *109*, 5649−5655.

(39) Bawendi, M. G.; Kortan, A. R.; Steigerwald, M. L.; Brus, L. E. X-Ray Structural Characterization of Larger CdSe Semiconductor Clusters. *J. Chem. Phys.* **1989**, *91*, 7282−7290.

(40) Steigerwald, M. L.; Brus, L. E. Semiconductor Crystallites: A Class of Large Molecules. *Acc. Chem. Res.* **1990**, *23*, 183−188.

(41) Bawendi, M. G.; Wilson, W. L.; Rothberg, L.; Carroll, P. J.; Jedju, T. M.; Steigerwald, M. L.; Brus, L. E. Electronic Structure and Photoexcited-Carrier Dynamics in Nanometer-Size CdSe Clusters. *Phys. Rev. Lett.* **1990**, *65*, 1623−1626.

(42) Wang, F.; Tang, R.; Buhro, W. E. The Trouble with TOPO; Iidentification of Adventitious Impurities Beneficial to the Growth of Cadmium Selenide Quantum Dots, Rods, and Wires. *Nano Lett.* **2008**, *8*, 3521−3524.

(43) Bawendi, M. G.; Steigerwald, M. L.; Brus, L. E. The Quantum Mechanics of Larger Semiconductor Clusters (" Quantum Dots"). *Annu. Rev. Phys. Chem.* **1990**, *41*, 477−496.

(44) Littau, K. A.; Szajowski, P. J.; Muller, A. J.; Kortan, A. R.; Brus, L. E. Luminescent Silicon Nanocrystal Colloid *via* a High Temperature Aerosol Reaction. *J. Phys. Chem.* **1993**, *97*, 1224−1230.

(45) Brus, L. E. The Luminescence of Silicon Materials: Chains, Sheets, Nanocrystals, Nanowires, Microcrystals, and Porous Silicon. *J. Phys. Chem.* **1994**, *98*, 3575−3581.

(46) Wilson, W. L.; Szajowski, P. F.; Brus, L. E. Quantum Confinement in Size-Selected, Surface Oxidized Silicon Nanocrystals. *Science* **1993**, *262*, 1242−1244.

(47) LaMer, V. K.; Dinegar, R. H. Theory, Production and Mechanism of Formation of Monodispersed Hydrosols. *J. Am. Chem. Soc.* **1950**, *72*, 4847−4854.

(48) Chemseddine, A.; Weller, H. Highly Monodisperse Quantum Sized CdS Particles by Size Selective Precipitation. *Ber, Bunsenges. Phys. Chem.* **1993**, *97*, 636−637.

(49) Kornowski, A.; Eichberger, R.; Giersig, M.; Weller, H.; Eychmüller, A. Preparation and Photophysics of Strongly Luminescing Cd_3P_2 Quantum Dots. *J. Phys. Chem.* **1996**, *100*, 12467−12471.

(50) Itoh, T.; Kirihara, T. Excitons in CuCl Microcrystals Embedded in NaCl. *J. Lumin.* **1984**, *31*−*32*, 120−122.

(51) Grigoryan, G. B.; Kazaryan, E. M.; Efros, Al. L.; Yazeva, T. V. Quantized Holes and the Absorption Edge in Spherical Semiconductor Microcrystals with a Complex Valence Band Structure. *Sov. Phys. Solid State* **1990**, *32*, 1031−1035.

(52) Norris, D. J.; Bawendi, M. G. Measurement and Assignment of the Size-Dependent Optical Spectrum in CdSe Quantum Dots. *Phys. Rev. B: Condens. Matter Mater. Phys.* **1996**, *53*, 16338−16346.

(53) Dingle, R.; Wiegmann, W.; Henry, C. H. Quantum States of Confined Carriers in Very Thin Al_xGa_{1-x}As-GaAs-Al_xGa_{1-x} Heterostructures. *Phys. Rev. Lett.* **1974**, *33*, 827−829.

(54) Brus, L. E. Model for Carrier Dynamics and Photoluminescence Quenching in Wet and Dry Porous Silicon Thin Films. *Phys. Rev. B: Condens. Matter Mater. Phys.* **1996**, *53*, 4649−4656.

(55) Marcus, R. A. Electrostatic Free Energy and Other Properties of States Having Nonequlibrium Polarization. *J. Chem. Phys.* **1956**, *24*, 979−989.

(56) Guo, Y.; Yaffe, O.; Hull, T.; Owen, J.; Reichman, D.; Brus, L. E. Dynamic Emission Stokes Shift and Liquid-Like Dielectric Solvation of Band Edge Carriers in Lead-Halide Perovskites. *Nat. Commun.* **2019**, *10*, 1175.

(57) Ritova, N. C. *Screened Potential of a Point Charge in a Thin Film.* Vestnik of Moskow University 1967, 30−36. Translated to English in *arXiv (Mesoscale and Nanoscale Physics)*, September 1, 2020, 1806.00976, ver. 2. https://arxiv.org/abs/1806.00976 (accessed 2020-09-01).

(58) Keldysh, L. V. Coulomb Interaction in Thin Semiconductor and Semimetal Films. *JETP Lett.* **1979**, *29*, 658−660.

(59) Hines, M. A.; Guyot-Sionnest, P. Synthesis and Characterization of Strongly Luminescing ZnS-Capped CdSe Nanocrystals. *J. Phys. Chem.* **1996**, *100*, 468−471.

(60) Talapin, D. V.; Mekis, I.; Gotzinger, S.; Kornowski, A.; Benson, O.; Weller, H. CdSe/CdS/ZnS and CdSe/ZnSe/ZnS Core-Shell-Shell Nanocrystals. *J. Phys. Chem. B* **2004**, *108*, 18826−18831.

(61) Lim, J.; Park, Y.-S.; Klimov, V. I. Optical Gain in Colloidal Quantum Dots Achieved with Direct-Current Electrical Pumping. *Nat. Mater.* **2018**, *17*, 42−49.

(62) Lifshitz, E.; Brumer, M.; Kigel, A.; Sashchiuk, A.; Bashouti, M.; Sirota, M.; Galun, E.; Burshtein, Z.; Le Quang, A. Q.; Ledoux-Rak, I.; Zyss, J. Air-Stable PbSe/PbS and PbSe/$PbSe_xS_{1-x}$ Core-Shell Nanocrystal Quantum Dots and Their Applications. *J. Phys. Chem. B* **2006**, *110*, 25356−25365.

(63) Won, Y.-H.; Cho, O.; Kim, T.; Chung, D.-Y.; Kim, T.; Chung, H.; Jang, H.; Lee, J.; Kim, D.; Jang, E. Highly Efficient and Stable InP/ZnSe/ZnS Quantum Dot Light-Emitting Diodes. *Nature* **2019**, *575*, 634−638.

(64) Heuer-Jungemann, A.; Feliu, N.; Bakaimi, I.; Hamaly, M.; Alkilany, A.; Chakraborty, I.; Masood, A.; Casula, M. F.; Kostopoulou, A.; Oh, E.; Susumu, K.; Stewart, M. H.; Medintz, I. L.; Stratakis, E.; Parak, W. J.; Kanaras, A. G. The Role of Ligands in the Chemical Synthesis and Applications of Inorganic Nanoparticles. *Chem. Rev.* **2019**, *119*, 4819−4880.

(65) Blanco-Canosa, J.; Wu, M.; Susumu, K.; Petryayeva, E.; Jennings, T. L.; Dawson, P. E.; Algar, W. R.; Medintz, I. L. Recent Progress in the Bioconjugation of Quantum Dots. *Coord. Chem. Rev.* **2014**, *263−264*, 101−137.

(66) Dorfs, D.; Eychmüller, A. Multishell Semiconductor Nanocrystals. In *Semiconductor nanocrystal quantum dots, synthesis, assembly, spectroscopy and applications*; Rogach, A. L., Ed.; Springer Nature: Switzerland, 2020; pp 101−117.

(67) Reiss, P.; Protière, M.; Li, L. Core/Shell Semiconductor Nanocrystals. *Small* **2009**, *5*, 154−168.

(68) Owen, J.; Brus, L. E. Chemical Synthesis and Luminescence Applications of Colloidal Semiconductor Quantum Dots. *J. Am. Chem. Soc.* **2017**, *139*, 10939−10343.

(69) Nirmal, M.; Dabbousi, B. O.; Bawendi, M. G.; Macklin, J. J.; Trautman, J. K.; Harris, T. D.; Brus, L. E. Fluorescence Intermittency in Single Cadmium Selenide Nanocrystals. *Nature* **1996**, *383*, 802−804.

(70) Murray, C. B.; Kagan, C. R.; Bawendi, M. G. Self-Organization of CdSe Nanocrystallites into Three-Dimensional Quantum Dot Superlattices. *Science* **1995**, *270*, 1335−1338.

(71) Boles, M. A.; Engel, M.; Talapin, D. V. Self-Assembly of Colloidal Nanocrystals: From Intricate Structures to Functional Materials. *Chem. Rev.* **2016**, *116*, 11220−11289.

(72) Ye, X.; Millan, J. A.; Engel, M.; Chen, J.; Diroll, B. T.; Glotzer, S. C.; Murray, C. B. Shape Alloys of Nanorods and Nanospheres from Self-Assembly. *Nano Lett.* **2013**, *13*, 4980−4988.

(73) Shevchenko, E. V.; Talapin, D. V.; Murray, C. B.; O'Brien, S. Structural Characterization of Self-Assembled Multifunctional Binary Nanoparticle Superlattices. *J. Am. Chem. Soc.* **2006**, *128*, 3620−3637.

(74) Boles, M. A.; Talapin, D. V. Many-Body Effects in Nanocrystal Superlattices: Departure from Sphere Packing Explains Stability of Binary Phases. *J. Am. Chem. Soc.* **2015**, *137*, 4494−4502.

(75) Peng, X.; Manna, L.; Yang, W.; Wickham, J.; Scher, E.; Kadavanich, A.; Alivisatos, A. P. Shape Control of CdSe Nanocrystals. *Nature* **2000**, *404*, 59−61.

(76) Shabaev, A.; Efros, Al. L. 1D Exciton Spectroscopy of Semiconductor Nanorods. *Nano Lett.* **2004**, *4*, 1821−1825.

(77) Katz, D.; Wizansky, T.; Millo, O.; Rothenberg, E.; Mokari, T.; Banin, U. Size-Dependent Tunneling and Optical Spectroscopy of CdSe Quantum Rods. *Phys. Rev. Lett.* **2002**, *89*, 086801.

(78) Sitt, A.; Hadar, I.; Banin, U. Band-Gap Engineering, Optoelectronic Properties and Applications of Colloidal Heterostructured Semiconductor Nanorods. *Nano Today* **2013**, *8*, 494−513.

(79) Hadar, I.; Philbin, J. P.; Panfil, Y. E.; Neyshtadt, S.; Lieberman, I.; Eshet, H.; Lazar, S.; Rabani, E.; Banin, U. Semiconductor Seeded Nanorods with Graded Composition Exhibiting High Quantum-Yield, High Polarization, and Minimal Blinking. *Nano Lett.* **2017**, *17*, 2524−2531.

(80) Jia, G.; Pang, Y.; Ning, J.; Banin, U.; Ji, B. Heavy-Metal-Free Colloidal Semiconductor Nanorods: Recent Advances and Future Perspectives. *Adv. Mater.* **2019**, *31*, 1900781.

(81) Manna, L.; Milliron, D. J.; Meisel, A.; Scher, E. C.; Alivisatos, A. P. Controlled Growth of Tetrapod-Branched Inorganic Nanocrystals. *Nat. Mater.* **2003**, *2*, 382−385.

(82) Bruchez, M., Jr; Moronne, M.; Gin, P.; Weiss, S.; Alivisatos, A. P. Semiconductor Nanocrystals as Fluorescent Biological Labels. *Science* **1998**, *281*, 2013−2016.

(83) Chan, W. C. W.; Nie, S. Quantum Dot Bioconjugates for Ultrasensitive Nonisotopic Detection. *Science* **1998**, *281*, 2016−2018.

(84) Dubertret, B.; Skourides, P.; Norris, D. J.; Noireaux, V.; Brivanlou, A. H.; Libchaber, A. *In Vivo* Imaging of Quantum Dots Encapsulated in Phospholipid Micelles. *Science* **2002**, *298*, 1759−1762.

(85) Bruns, O. T.; Bischof, T. S.; Harris, D. K.; Franke, D.; Shi, Y.; Riedemann, L.; Bartelt, A.; Jaworski, F. B.; Carr, J. A.; Rowlands, C. J.; Wilson, M. W. B.; Chen, O.; Wei, H.; Hwang, G. W.; Montana, D. M.; Coropceanu, I.; Achorn, O. B.; Kloepper, J.; Heeren, J.; So, P. T. C.; et al. Next-Generation *in Vivo* Optical Imaging with Short-Wave Infrared Quantum Dots. *Nature Biomed. Eng.* **2017**, *1*, 0056.

(86) Michalet, X.; Pinaud, F. F.; Bentolila, L. A.; Tsay, J. M.; Doose, S.; Li, J. J.; Sundaresan, G.; Wu, A. M.; Gambhir, S. S.; Weiss, S. Quantum Dots for Live Cells, *in Vivo* Imaging, and Diagnostics. *Science* **2005**, *307*, 538−544.

(87) Medintz, I. L.; Uyeda, H. T.; Goldman, E. R.; Mattoussi, H. Quantum Dot Bioconjugates for Imaging, Labelling and Sensing. *Nat. Mater.* **2005**, *4*, 435−446.

(88) Efros, Al. L.; Delehanty, J. B.; Huston, A. L.; Medintz, I. L.; Barbic, M.; Harris, T. D. Evaluating the Potential of Using Quantum Dots for Monitoring Electrical Signals in Neurons. *Nat. Nanotechnol.* **2018**, *13*, 278−288.

(89) Dameron, C.; Reese, R.; Mehra, R.; Kortan, A.; Carroll, P.; Steigerwald, M.; Brus, L. E.; Winge, D. Biosynthesis of Cadmium Sulphide Quantum Semiconductor Crystallites. *Nature* **1989**, *338*, 596−597.

(90) Norris, D. J.; Yao, N.; Charnock, F. T.; Kennedy, T. A. High-Quality Manganese-Doped ZnSe Nanocrystals. *Nano Lett.* **2001**, *1*, 3−7.

(91) Ekimov, A.I.; Kudryavtsev, I.A.; Ivanov, M.G.; Efros, Al. L. Spectra and Decay Kinetics of Radiative Recombination in CdS Microcrystals. *J. Lumin.* **1990**, *46*, 83−95.

(92) Norris, D. J.; Efros, Al. L.; Erwin, S. C. Doped Nanocrystals. *Science* **2008**, *319*, 1776−1779.

(93) Schimpf, A. M.; Knowles, K. E.; Carroll, G. M.; Gamelin, D. R. Electronic Doping and Redox-Potential Tuning in Colloidal Semiconductor Nanocrystals. *Acc. Chem. Res.* **2015**, *48*, 1929−1937.

(94) Knowles, K. E.; Hartstein, K. H.; Kilburn, T. B.; Marchioro, A.; Nelson, H. D.; Whitham, P. J.; Gamelin, D. R. Luminescent Colloidal Semiconductor Nanocrystals Containing Copper: Synthesis, Photophysics, and Applications. *Chem. Rev.* **2016**, *116*, 10820−10851.

(95) Qu, L.; Peng, Z. A.; Peng, X. Alternative Routes toward High Quality CdSe Nanocrystals. *Nano Lett.* **2001**, *1*, 333−337.

(96) Peng, Z. A.; Peng, X. Formation of High-Quality CdTe, CdSe, and CdS Nanocrystals Using CdO as Precursor. *J. Am. Chem. Soc.* **2001**, *123*, 183−184.

(97) Battaglia, D.; Peng, X. Formation of High Quality InP and InAs Nanocrystals in a Noncoordinating Solvent. *Nano Lett.* **2002**, *2*, 1027−1030.

(98) Yu, W. W.; Peng, X. Formation of High-Quality CdS and Other II-VI Semiconductor Nanocrystals in Noncoordinating Solvents: Tunable Reactivity of Monomers. *Angew. Chem., Int. Ed.* **2002**, *41*, 2368−2371.

(99) Peng, X. Green Chemical Approaches toward High-Quality Semiconductor Nanocrystals. *Chem. - Eur. J.* **2002**, *8*, 334−339.

(100) Jun, S.; Jang, E. Interfused Semiconductor Nanocrystals: Brilliant Blue Photoluminescence and Electroluminescence. *Chem. Commun.* **2005**, 4616−4618.

(101) Chen, Y.; Vela, J.; Htoon, H.; Casson, J. L.; Werder, D. J.; Bussian, D. A.; Klimov, V. I.; Hollingsworth, J. A. Giant" Multishell CdSe Nanocrystal Quantum Dots with Suppressed Blinking. *J. Am. Chem. Soc.* **2008**, *130*, 5026−5027.

(102) Chen, O.; Zhao, J.; Chauhan, V.; Cui, J.; Wong, C.; Harris, D.; Wei, H.; Han, H.-S.; Fukumura, D.; Jain, R.; Bawendi, M. G. Compact High-Quality CdSe-CdS Core-Shell Nanocrystals with Narrow Emission Linewidths and Suppressed Blinking. *Nat. Mater.* **2013**, *12*, 445−451.

(103) Cragg, G. E.; Efros, Al. L. Suppression of Auger Processes in Confined Structures. *Nano Lett.* **2010**, *10*, 313−317.

(104) Hendricks, M. P.; Campos, M. P.; Cleveland, G. T.; Jen-La Plante, I.; Owen, J. S. A. Tunable Library of Substituted Thiourea Precursors to Metal Sulfide Nanocrystals. *Science* **2015**, *348*, 1226−1230.

(105) Joo, J.; Son, J. S.; Kwon, S. G.; Yu, J. H.; Hyeon, T. Low-Temperature Solution-Phase Synthesis of Quantum Well Structured CdSe Nanoribbons. *J. Am. Chem. Soc.* **2006**, *128*, 5632−5633.

(106) Ithurria, S.; Dubertret, B. Quasi 2D Colloidal CdSe Platelets with Thicknesses Controlled at the Atomic Level. *J. Am. Chem. Soc.* **2008**, *130*, 16504−16505.

(107) Ithurria, S.; Tessier, M. D.; Mahler, B.; Lobo, R. P. S. M.; Dubertret, B.; Efros, Al. L. Colloidal Nanoplatelets with Two-Dimensional Electronic Structure. *Nat. Mater.* **2011**, *10*, 936−941.

(108) Achtstein, A. W.; Marquardt, O.; Scott, R.; Ibrahim, M.; Riedl, T.; Prudnikau, A. V.; Antanovich, A.; Owschimikow, N.; Lindner, J. K. N.; Artemyev, M.; Woggon, U. Impact of Shell Growth on Recombination Dynamics and Exciton-Phonon Interaction in CdSe-CdS Core-Shell Nanoplatelets. *ACS Nano* **2018**, *12*, 9476−9483.

(109) Tessier, M. D.; Spinicelli, P.; Dupont, D.; Patriarche, G.; Ithurria, S.; Dubertret, B. Efficient Exciton Concentrators Built from Colloidal Core/Crown CdSe/CdS Semiconductor Nanoplatelets. *Nano Lett.* **2014**, *14*, 207−213.

(110) Hazarika, A.; Fedin, I.; Hong, L.; Guo, J.; Srivastava, V.; Cho, W.; Coropceanu, I.; Portner, J.; Diroll, B. T.; Philbin, J. P.; Rabani, E.; Klie, R.; Talapin, D. V. Colloidal Atomic Layer Deposition with Stationary Reactant Phases Enables Precise Synthesis of "Digital" II-VI Nano - Heterostructures with Exquisite Control of Confinement and Strain. *J. Am. Chem. Soc.* **2019**, *141*, 13487−13496.

(111) Mews, A.; Eychmueller, A.; Giersig, M.; Schooss, D.; Weller, H. Preparation, Characterization, and Photophysics of the Quantum Dot Quantum Well System Cadmium Sulfide/Mercury Sulfide/Cadmium Sulfide. *J. Phys. Chem.* **1994**, *98*, 934−941.

(112) Son, D. H.; Hughes, S. M.; Yin, Y.; Alivisatos, A. P. Cation Exchange Reactions in Ionic Nanocrystals. *Science* **2004**, *306*, 1009−1012.

(113) Robinson, R. D.; Sadtler, B.; Demchenko, D. O.; Erdonmez, C. K.; Wang, L.-W.; Alivisatos, A. P. Spontaneous Superlattice Formation in Nanorods through Partial Cation Exchange. *Science* **2007**, *317*, 355−358.

(114) Casavola, M.; van Huis, M. A.; Bals, S.; Lambert, K.; Hens, Z.; Vanmaekelbergh, D. Anisotropic Cation Exchange in PbSe/CdSe Core/Shell Nanocrystals of Different Geometry. *Chem. Mater.* **2012**, *24*, 294−302.

(115) Boneschanscher, M. P.; Evers, W. H.; Geuchies, J. J.; Altantzis, T.; Goris, B.; Rabouw, F. T.; van Rossum, S. A. P.; van der Zant, H. S. J.; Siebbeles, L. D. A.; Van Tendeloo, G.; Swart, I.; Hilhorst, J.; Petukhov, A. V.; Bals, S.; Vanmaekelbergh, D. Long-Range Orientation and Atomic Attachment of Nanocrystals in 2D Honeycomb Superlattices. *Science* **2014**, *344*, 1377−1380.

(116) Sahu, A.; Kang, M. S.; Kompch, A.; Notthoff, C.; Wills, A. W.; Deng, D.; Winterer, M.; Frisbie, C. D.; Norris, D. J. Electronic Impurity Doping in CdSe Nanocrystals. *Nano Lett.* **2012**, *12*, 2587−2594.

(117) Mocatta, D.; Cohen, G.; Schattner, J.; Millo, O.; Rabani, E.; Banin, U. Heavily Doped Semiconductor Nanocrystal Quantum Dots. *Science* **2011**, *332*, 77−81.

(118) Galle, T.; Samadi Khoshkhoo, M.; Martin-Garcia, B.; Meerbach, C.; Sayevich, V.; Koitzsch, A.; Lesnyak, V.; Eychmuller, A. Colloidal PbSe Nanoplatelets of Varied Thickness with Tunable Optical Properties. *Chem. Mater.* **2019**, *31*, 3803−3811.

(119) Beberwyck, B. J.; Surendranath, Y.; Alivisatos, A. P. A Versatile Tool for Nanomaterials Synthesis. *J. Phys. Chem. C* **2013**, *117*, 19759−19770.

(120) Kovalenko, M. V.; Scheele, M.; Talapin, D. V. Colloidal Nanocrystals with Molecular Metal Chalcogenide Surface Ligands. *Science* **2009**, *324*, 1417−1420.

(121) Khabibullin, A. R.; Efros, Al. L.; Erwin, S. C. The Role of Ligands in Electron Transport in Nanocrystal Solids. *Nanoscale* **2020**, *12*, 23028−23035.

(122) Xu, J.; Voznyy, O.; Liu, M.; Kirmani, A. R.; Walters, G.; Munir, R.; Abdelsamie, M.; Proppe, A. H.; Sarkar, A.; de Arquer, F. P. G.; Wei, M.; Sun, B.; Liu, M.; Ouellette, O.; Quintero-Bermudez, R.; Li, J.; Fan, J.; Quan, L.; Todorovic, P.; Tan, H.; et al. 2D Matrix Engineering for Homogeneous Quantum Dot Coupling in Photovoltaic Solids. *Nat. Nanotechnol.* **2018**, *13*, 456−462.

(123) Gao, L.; Quan, L. N.; de Arquer, F. P. G.; Zhao, Y.; Munir, R.; Proppe, A.; Quintero-Bermudez, R.; Zou, C.; Yang, Z.; Saidaminov, M. I.; Voznyy, O.; Kinge, S.; Lu, Z.; Kelley, S. O.; Amassian, A.; Tang, J.; Sargent, E. H. Efficient Near-Infrared Light-Emitting Diodes Based on Quantum Dots in Layered Perovskite. *Nat. Photonics* **2020**, *14*, 227−233.

(124) Nenadovic, M. T.; Rajh, T.; Micic, O. I. Size Quantization in Small Semiconductor Particles. *J. Phys. Chem.* **1985**, *89*, 397−399.

(125) Borrelli, N. F.; Smith, D. W. Quantum Confinement of PbS Microcrystals in Glass. *J. Non-Cryst. Solids* **1994**, *180*, 25−31.

(126) Kang, I.; Wise, F. W. Electronic Structure and Optical Properties of PbS and PbSe Quantum Dots. *J. Opt. Soc. Am. B* **1997**, *14*, 1632−1646.

(127) Murray, C. B.; Sun, S.; Gaschler, W.; Doyle, H.; Betley, T. A.; Kagan, C. R. Colloidal Synthesis of Nanocrystals and Nanocrystal Superlattices. *IBM J. Res. Dev.* **2001**, *45*, 47−56.

(128) Schaller, R. D.; Klimov, V. I. High Efficiency Carrier Multiplication in PbSe Nanocrystals: Implications for Solar Energy Conversion. *Phys. Rev. Lett.* **2004**, *92*, 186601.

(129) Ellingson, R. J.; Beard, M. C.; Johnson, J. C.; Yu, P.; Micic, O. I.; Nozik, A. J.; Shabaev, A.; Efros, Al. L. Highly Efficient Multiple Exciton Generation in Colloidal PbSe and PbS Quantum Dots. *Nano Lett.* **2005**, *5*, 865−871.

(130) Saran, R.; Curry, R. Lead Sulphide Nanocrystal Photodetector Technologies. *Nat. Photonics* **2016**, *10*, 81−92.

(131) Colbert, A. E.; Placencia, D.; Ratcliff, E. L.; Boercker, J. E.; Lee, P.; Aifer, E. H.; Tischler, J. G. Enhanced Infrared Photodiodes Based on

PbS/PbCl$_x$ Core/Shell Nanocrystals. , *arXiv (Mesoscale and Nanoscale Physics)*, March 22, 2021, 2103.12006, ver. 1. https://arxiv.org/abs/2103.12006 (accessed 2021-03-22).

(132) Brus, L. E.; Szajowski, P. F.; Wilson, W. L.; Harris, T. D.; Schuppler, S.; Citrin, P. H. Electronic Spectroscopy and Photophysics of Si Nanocrystals: Relationship to Bulk c-Si and Porous Si. *J. Am. Chem. Soc.* **1995**, *117*, 2915−2922.

(133) Kovalev, D.; Heckler, H.; Ben-Chorin, M.; Polisski, G.; Schwartzkopff, M.; Koch, F. Breakdown of the Conservation Rule in Si Nanocrystals. *Phys. Rev. Lett.* **1998**, *81*, 2803−2806.

(134) Fadaly, E. M. T.; Dijkstra, A.; Suckert, J. R.; Ziss, D.; van Tilburg, M. A. J.; Mao, C.; Ren, Y.; van Lange, V. T.; Korzun, K.; Kölling, S.; Verheijen, M. A.; Busse, D.; Rödl, C.; Furthmüller, J.; Bechstedt, F.; Stangl, J.; Finley, J. J.; Botti, S.; Haverkort, J. E. M.; Bakkers, E. P. A. M. Direct-Bandgap Emission from Hexagonal Ge and SiGe Alloys. *Nature* **2020**, *580*, 205−209.

(135) Micic, O. I.; Curtis, C. J.; Jones, K. M.; Sprague, J. R.; Nozik, A. J. Synthesis and Characterization of InP Quantum Dots. *J. Phys. Chem.* **1994**, *98*, 4966−4969.

(136) Li, L.; Reiss, P. One-Pot Synthesis of Highly Luminescent InP/ZnS Nanocrystals without Precursor Injection. *J. Am. Chem. Soc.* **2008**, *130*, 11588−11589.

(137) Rogach, A.; Kershaw, S.; Burt, M.; Harrison, M.; Kornowski, A.; Eychmüller, A.; Weller, H. Colloidally Prepared HgTe Nanocrystals with Strong Room-Temperature Infrared Luminescence. *Adv. Mater.* **1999**, *11*, 552−555.

(138) Keuleyan, S.; Lhuillier, E.; Brajuskovic, V.; Guyot-Sionnest, P. Mid-Infrared HgTe Colloidal Quantum Dot Photodetectors. *Nat. Photonics* **2011**, *5*, 489−493.

(139) Lan, X.; Chen, M.; Hudson, M. H.; Kamysbayev, V.; Wang, Y.; Guyot-Sionnest, P.; Talapin, D. V. Quantum Dot Solids Showing State-Resolved Band-Like Transport. *Nat. Mater.* **2020**, *19*, 323−329.

(140) Protesescu, L.; Yakunin, S.; Bodnarchuk, M. I.; Krieg, F.; Caputo, R.; Hendon, C. H.; Yang, R. X.; Walsh, A.; Kovalenko, M. V. Nanocrystals of Cesium Lead Halide Perovskites (CsPbX$_3$, X = Cl, Br, and I): Novel Optoelectronic Materials Showing Bright Emission with Wide Color Gamut. *Nano Lett.* **2015**, *15*, 3692−3696.

(141) Rainò, G.; Nedelcu, G.; Protesescu, L.; Bodnarchuk, M. I.; Kovalenko, M. V.; Mahrt, R. F.; Stöferle, T. Single Cesium Lead Halide Perovskite Nanocrystals at Low Temperature: Fast Single-Photon Emission, Reduced Blinking, and Exciton Fine Structure. *ACS Nano* **2016**, *10*, 2485−2490.

(142) Kovalenko, M. V.; Protesescu, L.; Bodnarchuk, M. I. Properties and Potential Optoelectronic Applications of Lead Halide Perovskite Nanocrystals. *Science* **2017**, *358*, 745−750.

(143) Hanamura, E. Very Large Optical Nonlinearity of Semiconductor Microcrystallites. *Phys. Rev. B: Condens. Matter Mater. Phys.* **1988**, *37*, 1273−1279.

(144) Kayanuma, Y. Quantum-Size Effects of Interacting Electrons and Holes in Semiconductor Microcrystals with Spherical Shape. *Phys. Rev. B: Condens. Matter Mater. Phys.* **1988**, *38*, 9797−9805.

(145) Cho, K. Mechanisms for LT Splitting of Polarization Waves: A Link between Electron-Hole Exchange Interaction and Depolarization Shift. *J. Phys. Soc. Jpn.* **1999**, *68*, 683−691.

(146) Bryant, G. W. Excitons in Quantum Boxes: Correlation Effects and Quantum Confinement. *Phys. Rev. B: Condens. Matter Mater. Phys.* **1988**, *37*, 8763−8772.

(147) Sercel, P. C.; Vahala, K. J. Analytical Formalism for Determining Quantum-Wire and Quantum-Dot Band Structure in the Multiband Envelope-Function Approximation. *Phys. Rev. B: Condens. Matter Mater. Phys.* **1990**, *42*, 3690−3710.

(148) Takagahara, T. Excitonic Optical Nonlinearity and Exciton Dynamics in Semiconductor Quantum Dots. *Phys. Rev. B: Condens. Matter Mater. Phys.* **1987**, *36*, 9293−9296.

(149) Efros, Al. L.; Rosen, M. Quantum Size Level Structure of Narrow-Gap Semiconductor Nanocrystals: Effect of Band Coupling. *Phys. Rev. B: Condens. Matter Mater. Phys.* **1998**, *58*, 7120−7135.

(150) Lippens, P. E.; Lannoo, M. Calculation of the Band Gap for Small CdS and ZnS Crystallites. *Phys. Rev. B: Condens. Matter Mater. Phys.* **1989**, *39*, 10935−10942.

(151) Rama Krishna, M. V.; Friesner, R. A. Exciton Spectra of Semiconductor Clusters. *Phys. Rev. Lett.* **1991**, *67*, 629−632.

(152) Wang, L. W.; Zunger, A. Electronic Structure Pseudopotential Calculations of Large (.apprx.1000 Atoms) Si Quantum Dots. *J. Phys. Chem.* **1994**, *98*, 2158−2165.

(153) Nirmal, M.; Murray, C. B.; Bawendi, M. G. Fluorescence-Line Narrowing in CdSe Quantum Dots: Surface Localization of the Photogenerated Exciton. *Phys. Rev. B: Condens. Matter Mater. Phys.* **1994**, *50*, 2293−2300.

(154) Nirmal, M.; Norris, D. J.; Kuno, M.; Bawendi, M. G.; Efros, Al. L.; Rosen, M. Observation of the Dark Exciton in CdSe Quantum Dots. *Phys. Rev. Lett.* **1995**, *75*, 3728−3731.

(155) Norris, D. J.; Efros, Al. L.; Rosen, M.; Bawendi, M. G. Size Dependence of Exciton Fine Structure in CdSe Quantum Dots. *Phys. Rev. B: Condens. Matter Mater. Phys.* **1996**, *53*, 16347−16354.

(156) Efros, Al. L.; Rosen, M.; Kuno, M.; Nirmal, M.; Norris, D. J.; Bawendi, M. G. Band Edge Exciton in Quantum Dots of Semiconductor with a Degenerate Valence Band: Dark and Bright Exciton States. *Phys. Rev. B: Condens. Matter Mater. Phys.* **1996**, *54*, 4843−4856.

(157) Schmitt-Rink, S.; Miller, D. A. B.; Chemla, D. S. Theory of the Linear and Nonlinear Optical Properties of Semiconductor Microcrystallites. *Phys. Rev. B: Condens. Matter Mater. Phys.* **1987**, *35*, 8113−8124.

(158) Roussignol, P.; Ricard, D.; Lukasik, J.; Flytzanis, C. New Results on Optical Phase Conjugation in Semiconductor-Doped Glasses. *J. Opt. Soc. Am. B* **1987**, *4*, 5−13.

(159) Chepic, D.I.; Efros, Al. L.; Ekimov, A.I.; Ivanov, M.G.; Kharchenko, V.A.; Kudriavtsev, I.A.; Yazeva, T.V. Auger Ionization of Semiconductor Quantum Dots in Glass Matrices. *J. Lumin.* **1990**, *47*, 113−127.

(160) Kharchenko, V. A.; Rosen, M. Auger Relaxation Processes in Semiconductors Nanocrystals and Quantum Wells. *J. Lumin.* **1996**, *70*, 158−169.

(161) Klimov, V. I.; Mikhailovsky, A. A.; McBranch, D. W.; Leatherdale, C. A.; Bawendi, M. G. Quantization of Multiparticle Auger Rates in Semiconductor Quantum Dots. *Science* **2000**, *287*, 1011−1013.

(162) Efros, Al. L.; Nesbitt, D. J. Origin and Control of Blinking in Quantum Dots. *Nat. Nanotechnol.* **2016**, *11*, 661−671.

(163) Nozik, A. J. Quantum Dot Solar Cells. *Phys. E* **2002**, *14*, 115−120.

(164) Shabaev, A.; Efros, Al. L.; Nozik, A. J. Multiexciton Generation by a Single Photon in Nanocrystals. *Nano Lett.* **2006**, *6*, 2856−2863.

(165) Baer, R.; Rabani, E. Expeditious Stochastic Calculation of Multiexciton Generation Rates in Semiconductor Nanocrystals. *Nano Lett.* **2012**, *12*, 2123−2128.

(166) Shabaev, A.; Hellberg, C. S.; Efros, Al. L. Efficiency of Multiexciton Generation in Colloidal Nanostructures. *Acc. Chem. Res.* **2013**, *46*, 1242−1251.

(167) Zohar, G.; Baer, R.; Rabani, E. Multiexciton Generation in IV-VI Nanocrystals: The Role of Carrier Effective Mass, Band Mixing, and Phonon Emission. *J. Phys. Chem. Lett.* **2013**, *4*, 317−322.

(168) Semonin, O. E.; Luther, J. M.; Choi, S.; Chen, H. Y.; Gao, J.; Nozik, A. J.; Beard, M. C. Peak External Photocurrent Quantum Efficiency Exceeding 100% *via* MEG in a Quantum Dot Solar Cell. *Science* **2011**, *334*, 1530−1533.

(169) Beard, M. C.; Luther, J. M.; Semonin, O. E.; Nozik, A. J. Third Generation Photovoltaics Based on Multiple Exciton Generation in Quantum Confined Semiconductors. *Acc. Chem. Res.* **2013**, *46*, 1252−1260.

(170) Brus, L. E. Size, Dimensionality, and Strong Electron Correlation in Nanoscience. *Acc. Chem. Res.* **2014**, *47*, 2951−2959.

(171) Bartnik, A. C.; Efros, Al. L.; Koh, W.-K.; Murray, C. B.; Wise, F. W. Electronic States and Optical Properties of PbSe Nanorods and Nanowires. *Phys. Rev. B: Condens. Matter Mater. Phys.* **2010**, *82*, 195313.

(172) Benchamekh, R.; Gippius, N. A.; Even, J.; Nestoklon, M. O.; Jancu, J.-M.; Ithurria, S.; Dubertret, B.; Efros, Al. L.; Voisin, P. Tight-Binding Calculations of Image-Charge Effects in Colloidal Nanoscale Platelets of CdSe. *Phys. Rev. B: Condens. Matter Mater. Phys.* **2014**, *89*, 035307.

(173) Yang, J.; Wise, F. W. Electronic States of Lead-Salt Nanosheets. *J. Phys. Chem. C* **2015**, *119*, 26809−26816.

(174) Kovalev, D.; Chorin, M. B.; Diener, J.; Koch, F.; Efros, Al. L.; Rosen, M.; Gippius, N. A.; Tikhodeev, S. G. Porous Si Anisotropy from Photoluminescence Polarization. *Appl. Phys. Lett.* **1995**, *67*, 1585−1587.

(175) Rodina, A. V.; Efros, Al. L. Effect of Dielectric Confinement on Optical Properties of Colloidal Nanostructures. *J. Exp. Theor. Phys.* **2016**, *122*, 554−566.

(176) Rashba, E. I.; Gurgenishvili, G. E. Edge Absorption Theory in Semiconductors. *Sov. Phys. Solid State* **1962**, *4*, 759−760.

(177) Itoh, T.; Furumiya, M.; Ikehara, T.; Gourdon, C. Size-Dependent Radiative Decay Time of Confined Excitons in CuCl Microcrystals. *Solid State Commun.* **1990**, *73*, 271−274.

(178) Becker, M. A.; Vaxenburg, R.; Nedelcu, G.; Sercel, P. C.; Shabaev, A.; Mehl, M. J.; Michopoulos, J. G.; Lambrakos, S. G.; Bernstein, N.; Lyons, J. L.; Stöferle, T.; Mahrt, R. F.; Kovalenko, M. V.; Norris, D. J.; Rainò, G.; Efros, Al. L. Bright Triplet Excitons in Caesium Lead Halide Perovskites. *Nature* **2018**, *553*, 189−193.

(179) Zhou, J.; Zhu, M.; Meng, R.; Qin, H.; Peng, X. Ideal CdSe/CdS Core/Shell Nanocrystals Enabled by Entropic Ligands and Their Core Size-, Shell Thickness-, and Ligand-Dependent Photoluminescence Roperties. *J. Am. Chem. Soc.* **2017**, *139*, 16556−16567.

(180) Liu, Z.; Lin, C.-H.; Hyun, B.-R.; Sher, C.-W; Lv, Z.; Luo, B.; Jiang, F.; Wu, T.; Ho, C.-H.; Kuo, H.-C.; He, J.-H. Micro-Light-Emitting Diodes with Quantum Dots in Display Technology. *Light: Sci. Appl.* **2020**, *9*, 85.

(181) Kagan, C. R. Flexible Colloidal Nanocrystal Electronics. *Chem. Soc. Rev.* **2019**, *48*, 1626−1641.

(182) Kagan, C. R.; Bassett, L. C.; Murray, C. B.; Thompson, S. M. Colloidal Quantum Dots as Platforms for Quantum Information Science. *Chem. Rev.* **2021**, *121*, 3186−3233.

(183) Roh, J.; Park, Y.-S.; Lim, J.; Klimov, V. I. Optically Pumped Colloidal-Quantum-Dot Lasing in LED-Like Devices with an Integrated Optical Cavity. *Nat. Commun.* **2020**, *11*, 271.